JPET Fast Forward. Published on March 13, 2019 as DOI: 10.1124/jpet.118.255729
This article has not been copyedited and formatted. The final version may differ from this version.

JPET # 255729

Inhibition **of methamphetamine self-administration and reinstatement by central blockade of angiotensin II receptor in rats**

[1]Xing Xu, [1]Jian Pan, [2]Xingxing Li, [3]Yan Cui, [1]Zijuan Mao, [1]Boliang Wu, [3]Huachong Xu, [1,4]Wenhua Zhou, [1]Yu Liu

[1] Ningbo University School of Medicine, 818 Fenghua Road, Ningbo, Zhejiang 315211, P. R. China

[2] Ningbo Kangning Hospital, 1 South Zhuangyu Road, Ningbo, Zhejiang 315201, P. R. China.

[3] Ningbo Public Security Bureau Ningbo Anti-drug Office, 36 Xibei Road, Zhejiang 315040, P. R. China

[4] Ningbo Addiction Research and Treatment Center, 21 Xibei Road, Zhejiang 315040, P. R. China

JPET Fast Forward. Published on March 13, 2019 as DOI: 10.1124/jpet.118.255729
This article has not been copyedited and formatted. The final version may differ from this version.

JPET # 255729

Running title: AT1R blockade of methamphetamine self-administration in rats

Corresponding author: Yu Liu, Ningbo University School of Medicine, 818 Fenghua Road, Ningbo 315211, Zhejiang, P. R. China, Tel: 86-574-87600761, Fax: 86-574-87345902, Email: liuyu@nbu.edu.cn

Text pages: 31; **Tables**: 1; **Figures**: 9; **References**: 64; **Abstract**: 228 words; **Introduction**: 698 words; **Discussion**: 1488 words

List of non-standard abbreviations: Methamphetamine: METH; Angiotensin II receptor: ATR; Angiotensin II receptor type 1: AT1R; Candesartan cilexetil: CAN; self-administration: SA; Dopamine D2 receptor: D2R; Nucleus accumbens: NAc; Fixed ratio 1:FR1, Progressive ratio: PR; cAMP responsive element-binding protein: CREB; Phospholipase C beta: PLCβ; Beta Actin: β-actin; PBS, phosphate buffered saline;

PVDF, polyvinylidene difluoride; DMEM, Dulbecco's modified Eagle's medium; SEM, standard error of mean

A recommended section assignment: behavioral pharmacology

JPET Fast Forward. Published on March 13, 2019 as DOI: 10.1124/jpet.118.255729
This article has not been copyedited and formatted. The final version may differ from this version.

Abstract

The molecular mechanism and treatment of methamphetamine (METH) use disorder remain unclear. The current study aimed to investigate the role of central angiotensin II receptor (ATR) in drug taking and seeking behavior associated with METH use disorder. The effect of an angiotensin II receptor type 1 (AT1R) antagonist, candesartan cilexetil (CAN), on the reinforcing and motivational effects of METH was firstly assessed, using the animal model of METH self-administration (SA) and reinstatement. The level of dopamine D2 receptor (D2R) and AT1R was subsequently examined. Furthermore, the present study determined the expression of microRNAs by comparing METH SA, METH-yoked and saline-yoked groups. The target microRNAs were further overexpressed in the nucleus accumbens (NAc) via a lentivirus vector to investigate the effects of target microRNAs on METH SA maintained under a fixed ratio 1 (FR1), progressive ratio (PR) and cue-/drug-reinstatement of METH SA. The potential role of AT1R-PLCβ-CREB signaling pathway was finally investigated. The results suggest that AT1R blockade effectively reduced METH SA and reinstatement, in conjunction with counter-regulation of D2R and AT1R. A total of 17 miRNAs targeting AngII in NAc were found to be associated with voluntary intake of METH. Furthermore, overexpression of specific miR-219a-5p targeting AT1R regulated METH SA and reinstatement. The AT1R-PLCβ-CREB signaling pathway was found to be associated with the effect of AT1R on the drug-taking and seeking behavior involving METH use disorder.

Key words

Methamphetamine use disorder, self-administration, angiotensin II receptor type 1, microRNA, PLCβ,

Introduction

Methamphetamine (METH) use disorder has resulted in major public health problems worldwide (Fulcher et al., 2018; Gao et al., 2018; Krizman-Matasic et al., 2018). In addition to compulsive drug taking and seeking behavior, individuals with METH use disorder commonly present with other comorbidities, including cognitive deficits, depression, psychosis, anxiety and sleep disorders (Grant et al., 2012; McKetin et al., 2013; Mullen and Crawford, 2018). These comorbid disorders may further deteriorate the complex consequences of METH use disorder, supporting the need for "trans-diagnostic treatment approaches" (Bernheim et al., 2016; Hartel-Petri et al., 2017). Given that no medications have demonstrated a convincing and consistent effect to treat METH use disorder, an increasing number of studies have highlighted the potential use of medications targeting cognitive impairments associated with executive function for METH use disorder (Sofuoglu et al., 2013). Cholinesterase inhibitors (e.g., galantamine and rivastigmine) and monoamine transporter inhibitors (e.g., modafinil and methylphenidate) have shown promising effects to improve the treatment outcomes of METH use disorder (Sofuoglu et al., 2013; Franke et al., 2014).

Early studies demonstrated an independent renin angiotensin system (RAS) in the central nervous system (Basmadjian et al., 2017). The central binding sites of Angiotensin II (Ang II) have been identified in the cortex, hippocampus and midbrain (Wright and Harding, 1994; Holme et al., 2018). In the central nervous system, an

JPET Fast Forward. Published on March 13, 2019 as DOI: 10.1124/jpet.118.255729
This article has not been copyedited and formatted. The final version may differ from this version.

abundant increase of Ang II is associated with neuroinflammation, neuronal damage and neurodegeneration. Ang II has two different subtypes of cell-surface receptors, Ang II receptor type 1 (AT1R) and Ang II receptor type 2 (ATR2). Brain Ang II, mainly through AT1R, has also been demonstrated to interact with dopaminergic, glutamatergic and GABAergic neurotransmission in the brain (Basmadjian et al., 2017). AT1R blockade has been suggested to be a therapeutic target for the cognitive deficits associated with a wide range of central nervous system disorders, including Alzheimer's disease, human immunodeficiency virus infection, neuropathic pain, Parkinson's disease, schizophrenia, and depression (Muthuraman and Kaur, 2016; Saavedra, 2016; Zhuang et al., 2016; Erlandson et al., 2017; Fan et al., 2017; Perez-Lloret et al., 2017; Vian et al., 2017).

A limited number of studies have begun to explore the role of central Ang II and AT1R on the behavioral consequences of drugs of abuse. For example, AT1R in the central nucleus of the amygdala has been shown to involve the hemodynamic responses to cocaine in rats (Knuepfer et al., 2005; Watanabe et al., 2010). Blockade of AT1R by losartan enabled to elevate cocaine-induced hemodynamic responses in rats (Watanabe et al., 2010). Multiple doses of METH significantly unregulated the expression of AT1R in the striatum of mice, along with decreased dopamine D3 receptor expression (Jiang et al., 2018). The inhibition or genetic deletion of AT1R was sufficient to attenuate the hyperlocomotion induced by METH and amphetamine in mice (Jiang et al., 2018). An increased AT1R density induced by 21 days of

amphetamine injections was evident in both caudate putamen and NAc of mice. In contrast, desensitized response of AT1R to Ang II has also been reported in rats with repeated injections of amphetamine (Casarsa et al., 2015). However, direct microinjection of Ang II in the rat VTA and NAc significantly lowered morphine self-administration (SA) (Hosseini et al., 2007; Hosseini et al., 2009). In addition, the injection of Ang II into the NAc failed to alter morphine-induced conditional place preference in rats (Hosseini et al., 2007).

The majority of the previously described studies have used passive administration of drugs of abuse and an animal model of behavioral sensitization. Drug use disorder is characterized by a compulsion to seek and use drugs, a loss of control over intake, and repeated episodes of relapse (Cami and Farre, 2003). Up to date, the effect of central ATR1 and Ang II system on the addictive properties of drugs has not been reported in the literature. The current study is designed to evaluate the role of Ang II and AT1R in the addictive aspects of METH, using the animal model of METH SA and cue-/drug- induced reinstatement. A specific miRNA that targeted AT1R was also identified in the current study. The potential role of AT1R-PLCβ-CREB signaling pathway in the effect of AT1R blockade on METH was finally investigated.

Materials and methods

Animals

Male Sprague-Dawley (SD) rats (Zhejiang Academy of Medical Sciences, Hangzhou,

Zhejiang, China) weighing approximately 300-350g at the beginning of the experiment were individually housed under a standard environment (temperature, 23±1°C; humidity, 40-70%) with a 12:12 hour light/dark cycle (lights off at 07:00, on at 19:00). Food and water were provided abundantly. The experimental protocol was approved by an Institutional Review Committee for the use of Animal Subjects. All the experiments were conducted in accordance with the guidelines of the Institutional Laboratory Animal Care and Use of Ningbo University.

Drugs

METH (>90% purity) was provided by Ningbo Anti-drug Bureau of Ningbo Police and dissolved in physiological saline. The purity of METH was measured by High-performance liquid chromatography. The mobile phase contained KH_2PO_4 buffer (50 mmol/L, PH=3.0) and acetonitrile (70:30, v/v%). The flow rate was 1 ml/min. The column was Phenomenex Luna 5u SCX 100A, 250 mm X 4.6 mm, 5 um. The measured wavelengths were 215 nm. The wavelengths with the range of 190-360nm were collected. The retention time was 11 minutes. The sample was dissolved in the mobile phase and the concentration was 1.0 mg/ml. The injection volume was 20ul for all measurements. The measurement of each sample was carried out six times. Candesartan Cilexetil (CAN, (TCV-116), Tokyo Chemical Industry, Japan) was dissolved in 100% DMSO and administered in an oral gavage route.

Surgery

JPET Fast Forward. Published on March 13, 2019 as DOI: 10.1124/jpet.118.255729
This article has not been copyedited and formatted. The final version may differ from this version.

The animals were anesthetized with 1.5% sodium pentobarbital (30 mg/kg) and 0.03 ml xylazine hydrochloride. Each animal was implanted with a silastic catheter in the jugular vein. The catheter was passed subcutaneously to a polyethylene assembly mounted on the animal's back. The catheters were flushed daily with sterile saline containing heparin sodium (0.4%) and penicillin sodium to maintain catheter patency and prevent infection.

METH SA

Rats were permitted at least 3 days of recovery from the surgery before behavioral training was conducted. Rats were trained to respond on an active hole to receive METH infusions. A nose-poke response in the left (active) hole was immediately reinforced with an injection of METH. A nose-poke response in the right (inactive) hole was considered as an inactive response which had no programmed consequences. And if the active hole was activated, METH infusion was delivered through a fixed ratio 1 (FR1) reinforcement schedule. In each FR1 session, each nose-poke response in the active hole resulted in the delivery of 0.5 mg/kg/infusion METH (0.0175 ml injection volume delivered for 3.966s) and initiated a 20-sec time-out period in which active lever presses were counted but failed to result in METH delivery. If an inactive hole was activated, there were no programmed consequences. Daily FR1 training sessions lasted 4 hours or until 200 METH infusions were self-administered in one session, whichever came first. Following the acquisition, rats were allowed to self-administer METH under the FR1 and progressive ratio (PR) schedule. The PR

schedule of reinforcement was introduced following the FR1 testing. Briefly, each daily PR session was 6 hours in duration. On the PR schedule, a progressively increasing number of responses (1, 2, 4, 6, 9, 12, 15, 20, 25, 32, 40, 50, 62, 77, 95, 118, 145,178, 219, 268, 328, 402, 492, and 603) were required for the next METH infusion. Breakpoints were defined as the number of total injections following last obtained injection which was prior to a 1-hour period of non-reinforcement. Prior to drug testing, breakpoints maintained by METH were generated from at least three consecutive sessions of stable responding.

Yoked METH SA and saline procedure

Both yoked METH SA (yoked-METH） and yoked saline (yoked-saline) groups were tested simultaneously as METH SA group in different conditions. Either yoked-METH or yoked-saline rat was paired with one METH SA rat. Yoked-METH rats received the intravenous infusions of METH at the same dose, number and rate as the METH SA group. Yoked-saline group received the intravenous infusions of saline at the same number and rate as the METH SA group. The nose pokes by the yoked rats were recorded but had no programmed consequences.

Cue- and drug-induced reinstatement of METH SA

Following METH SA, the animals were subjected to extinction for 7 days. During the extinction phase, the animals were placed in chambers, which were similar to those for METH SA. However, the METH-associated stimuli (cue lights or noise) were not

JPET Fast Forward. Published on March 13, 2019 as DOI: 10.1124/jpet.118.255729
This article has not been copyedited and formatted. The final version may differ from this version.

presented, and no infusions were delivered. After extinction, the cue- or drug-induced reinstatement test was introduced. The cue-induced reinstatement test began with the non-contingent presentation of drug-associated cues including house-light and pump sound. During the experiment of cue-induced METH SA reinstatement, the light and sound cues were the same as those used during the period of METH SA acquisition. The only difference between self-administration and the cue-induced reinstatement test was that drug solution was not infused during reinstatement. The drug-induced reinstatement, rats were treated with an i.p. injection of METH (10mg/kg). After 30 minutes, rats were placed in chambers in which METH-associated stimuli were presented and METH infusions were substituted with saline.

μParaflo™ MicroRNA microarray Assay(Li et al., 2016)

Microarray assay was performed using a service provider (LC Sciences). In the assay, RNA sample with 4 to 8 μg were 3'-extended with a poly(A) tail using poly(A) polymerase. For the following fluorescent dye staining, an oligonucleotide tag was ligated to the poly(A) tail. A micro-circulation pump (Atactic Technologies) was used for hybridization which was performed overnight on a μParaflo microfluidic chip. On the microfluidic chip, each detection probe consisted of a chemically modified nucleotide coding segment. The segment was complementary to the target microRNA (from miRBase, http://www.mirbase.org/) or other RNA (control or customer defined sequences). A spacer segment of polyethylene glycol was used to extend the coding segment away from the substrate. PGR (photogenerated reagent) chemistry was

JPET Fast Forward. Published on March 13, 2019 as DOI: 10.1124/jpet.118.255729
This article has not been copyedited and formatted. The final version may differ from this version.

applied to prepare the detection probes via in situ synthesis. Chemical modifications of the detection probes were used to balance the hybridization melting temperatures. During the process of hybridization, 100 L6xSSPE buffer (0.90 M NaCl, 60 mM Na_2HPO_4, 6 mM EDTA, pH 6.8) containing 25% formamide at 34° was applied. Subsequently, tag-conjugating Cy3 dye was circulated through the microfluidic chip for dye staining. Fluorescence images were obtained by a laser scanner (GenePix 4000B, Molecular Device) and analyzed by the Array-Pro image analysis software (Media Cybernetics). Data were analyzed by first subtracting the background and then normalizing the signals using a LOWESS filter (locally weighted regression).

Quantitative Real-Time PCR (qPCR) Analyses

miRNA RT-qPCR analysis was performed using a Hairpin-itTM microRNA RT-PCR Quantitation Kit v1406 (GenePharma, China). All reactions were run in triplicate, and the results were normalized to those for miR-219a-5p. Amplification was performed using a reaction cycle at 95°C for 3 min, 95°C for 12 sec, and 62°C for 40 sec. The fluorescence signal was detected at the end of each cycle. The relative miRNA production was determined using the $2^{-\Delta Ct}$ method, where Ct is the threshold cycle. Total RNA was extracted from Hip/ VTA/ NAc/ PFC and CPU tissues, using Trizol reagent (Invitrogen, Carlsbad, CA). cDNA was generated from 1000ng mRNA with a SuperScript II Reverse Transcriptase kit and random oligonucleotides (Invitrogen, Carlsbad, CA). Measured mRNA abundance was normalized to β-actin and expressed as fold change relative to the vehicle control group. All primer sequences

are listed in Supplemental file (Supplemental Table 1).

Intracerebral injection procedures

The animals were anesthetized using 1.5% sodium pentobarbital (30 mg/kg) and 0.03 ml xylazine hydrochloride. The animals were positioned in a stereotaxic frame (Shenzhen Ruiwoode Life Technology Co., Ltd.). A total of 6 viral supernatant injections (1 µl per injection; viral supernatant concentrations ranged from 6.8×10^7 – 1×10^8 infection units/ml) were administered into each side of the NAc. Each rat received a total of 6 NAc injections(Im et al., 2010). The viruses were delivered toward the core (AcbC) and shell (AcbSh) portions of the NAc. The injections on the AcbC were given based on the following stereotaxic coordinates: anterior/posterior (AP): 1.20 mm from the bregma; medial/lateral (ML): ±1.40 mm and ±2.40 mm from midline; dorsal/ventral (DV): −6.6 and −7.2 mm below the dura. The injections on the AcbSh were given based on the following stereotaxic coordinates: AP: 1.20 mm from the bregma; ML: ±1.40 mm from the midline; DV: −7.9 mm below the dura. A small hole was drilled through the skull and the virus was delivered through a stainless-steel injection. The duration of viral supernatant injection was over 60 sec. Following the infusion, the injector remained in place for an additional 60 sec. The injector was then raised to the next more dorsal injection site, and the procedure was repeated. Finally, the holes were filled with polyethylene, and the animals were treated with penicillin sodium to prevent infection.

Western blotting

The brains were rapidly removed after the behavioral experiments and dissected to obtain the Hip/ VTA/ NAc/ PFC and CPU. The tissue was homogenized on ice in an ice-cold mixture of PMSF and RIPA lysis buffer (1:100). The homogenates were centrifuged at 16,000 rpm at 4°C for 30 min, and the concentrations of protein were determined using the Pierce BCA Protein Assay Kit. Equal concentrations of protein were diluted using PBS and 5x loading buffer. The protein was separated via SDS-PAGE and transferred to a PVDF membrane (Bio-Rad Laboratories). The PVDF membranes were blocked in 5% non-fat dried milk in Tris-buffered saline (TBS) that contained 0.05% Tween for 3 hours. The membranes were incubated at 4°C overnight with following primary antibodies: Anti-Angiotensin II Type 1 Receptor (AT1R ,1:1000; ab18801, Abcam), Anti-Dopamine D2 Receptor (D2R, 1:5000; ab85367, Abcam), Anti- cAMP responsive element-binding protein (CREB, 1:1000, Cat. No. 4820, Cell Signaling Technology), Anti-Phospholipase C beta 1 (PLCβ,1:1000, ab182359, Abcam) and Anti-beta Actin (β-actin, ab8226, 1:5000) overnight at a temperature of 4°C. The samples were rinsed a total of four times (each 10 min) using TBST solutions. The secondary antibody used was goat (polyclonal) anti-rabbit IgG (1:15,000; LI-COR Bioscience). The samples were incubated with the corresponding second antibodies at room temperature for 2 h. The samples were also rinsed a total of four times using the TBST solutions (10 min each time). The samples were developed using ECL chemiluminescence reagent (Thermo Scientific), Immunoreactivity was detected using the Odyssey Imaging System Application

JPET Fast Forward. Published on March 13, 2019 as DOI: 10.1124/jpet.118.255729
This article has not been copyedited and formatted. The final version may differ from this version.

(Odyssey, USA).

Cell Culture

Rat pheochromocytoma (PC12) cells were obtained from the Chinese Academy of Sciences (Shanghai, China) and cultured in high glucose modified Eagle's medium (DMEM) that contained 10% fetal bovine serum (FBS) and penicillin (100 U/ml)/streptomycin (100 μg/ml). The cells were cultured in an incubator at 37℃ and 5% CO_2. The culture medium was replaced every 2 days, and cells at the logarithmic growth phase were obtained for subsequent experiments.

Experimental Procedures

Experiment 1: The effect of AT1R blockade on METH SA and cue-/drug- induced reinstatement

Following acquisition, rats self-administered METH on the FR1 and PR schedule. Five doses of METH (0.025, 0.05, 0.075, and 0.1 mg/kg/infusion) were tested using a *Latin square design*. Saline was given prior to DMSO and CAN testing. Rats were divided into Saline+METH (n=9), DMSO+METH (n=8), 5CAN+METH (n=7), and 10CAN+METH (n=7). The effects of vehicle (DMSO) administration were also examined on the day immediately prior to and following one dose of CAN testing. Two doses of CAN (5mg/kg and 10mg/kg) were tested in a random order. In all tests, DMSO and CAN was administered 120 minutes prior to the initiation of SA sessions. Rats were decapitated 2 hours after saline, DMSO, 5CAN or 10CAN testing. The level

JPET Fast Forward. Published on March 13, 2019 as DOI: 10.1124/jpet.118.255729
This article has not been copyedited and formatted. The final version may differ from this version.

of D2R and AT1R was detected in the caudate putamen (CPU), Hippocampus (Hip), NAc, prefrontal cortex (PFC) and ventral tegmental area (VTA). Following the acquisition of METH SA, rats were maintained on 0.05 mg/kg/infusion of METH under the FR1 schedule for 14 days. One additional group of rats self-administered saline during the same period of time. Based on their performance on the last three days of METH SA (number of infusions per session), METH SA rats were divided into five groups (METH SA, Saline, DMSO, 5CAN and 10CAN). Rats in the METH SA were decapitated 2 hours immediately after the last SA session. The level of D2R and AT1R was detected in the CPU, Hip, NAc, PFC and VTA. Rats in the saline (n=6), DMSO (n=7), 5CAN (n=7) and 10CAN (n=8) group underwent additional 7 days of extinction. On the first day after extinction, each group of rats received saline, DMSO, 5mg/kg, or 10 mg/kg of CAN, respectively. After 120 minutes, half of rats were placed in the operant chamber for cue-induced reinstatement of METH SA. Half of rats received an i.p injection of METH 30 minutes prior to being placed in the operant chamber for drug-induced reinstatement of METH SA. After an additional 7 days of abstinence, all the animals received the same vehicle or CAN on the second trial as the first. Rats which were firstly on the cue-induced reinstatement testing were switched to drug-induced reinstatement testing and *vice versa*. Rats were decapitated 2 hours after cue- or drug-induced reinstatement testing. The level of D2R and AT1R was detected in the CPU, Hip, NAc, PFC and VTA.

Experiment 2: The effect of METH SA on the expression of NAc miRNA

JPET Fast Forward. Published on March 13, 2019 as DOI: 10.1124/jpet.118.255729
This article has not been copyedited and formatted. The final version may differ from this version.

Following METH acquisition, a total of 12 rats self-administered 0.05mg/kg/infusion of METH under the FR1 schedule for 14 days. Two additional groups were yoked-METH (n=12) and yoked-saline (n=12) groups described previously. Two hours after the behavioral testing was completed, NAc was isolated from whole brain and the expression of microRNA was examined. The findings of miR-219a-5p were further validated by RT-qPCR.

Experiment 3: The effect of miRNA 219a-5p overexpression on METH SA and cue-/drug- induced reinstatement

Rats were trained to self-administer METH and a dose response curve of METH SA (0.025, 0.05, 0.075 and 0.100 mg/kg/infusion) was generated as the baseline for all the animals. Based on the baseline, the animals were further divided into two groups (LV1NC and LV1-miR-219a-5p). Rats were infused with lentiviruses as control (LV1NC; n=6) or lentiviruses containing miR-219a-5p (LV1-miR-219a-5p; n=7) into NAc and then tested on various doses of METH maintained by FR1 and PR schedule. The animals were decapitated 2 hours immediately after the SA session. Relative expression of NAc miR-219a-5p was also identified in rats self-administering METH under FR1 or PR schedule. The level of AT1R, the primary phospholipase (PLCβ) and cAMP-response element binding protein (CREB) was also detected in the same group of animals. Additional rats self-administered 0.05 mg/kg/infusion METH under the FR1 schedule for 14 days. Based on their performance on the last three days of METH SA (number of infusions per session), rats were divided into two groups

(LV1NC, n=8; LV1-miR-219a-5p, n=7). During the period of abstinence, rats were infused with lentiviruses (LV1NC) or lentiviruses containing miR-219a-5p (LV1-miR-219a-5p) into NAc. Half of the animals were then tested on cue-induced reinstatement of METH SA and were switched to drug-induced reinstatement of METH SA following additional 7 days of abstinence. The other half of the animals were firstly tested on drug-induced reinstatement and then switched to cue-induced reinstatement of METH SA. The animals were decapitated 2 hours immediately after the reinstatement session. Relative expression of NAc miR-219a-5p was also identified in rats on either cue- or drug-induced reinstatement of METH SA. The level of AT1R, PLCβ and CREB was also detected in the same group of animals.

Experiment 4: The potential role of AT1R-PLCβ-CREB signaling pathway in the effect of AT1R on METH SA

The relative protein expression and mRNA expression of ATR1, PLCβand CREB was identified in rat pheochromocytoma (PC12) cells. PC12 cells were seeded onto 6-well plates and treated with 2.0 mM METH and different doses of CAN (2.5, 5.0, 10.0 and 20.0μM). The total RNA from PC12 cell in Trizol reagent was determined by Multiskan Go (Thermo Scientific, Waltham, MA, USA) after METH exposure for 24 hours. Real-time PCR was performed according to the manufacturer's instructions (TRANSGEN, AQ101). Sequences of primers were listed in Supporting Information Table S1, The PCR reaction conditions were as follows: 94 °C for 30 sec, 45 cycles at 94 °C for 5 sec ,60 °C for 15 sec and 72 °C 10 sec. PC12 cells were homogenized

JPET Fast Forward. Published on March 13, 2019 as DOI: 10.1124/jpet.118.255729
This article has not been copyedited and formatted. The final version may differ from this version.

using RIPA buffer (1:10) in which cocktail inhibitors and mercaptoethanol were freshly added. Protein concentrations were measured using the BCA protein assay kit (Thermo Scientific, Waltham, MA). 25 μg of protein was loaded on the gel. After electrophoresis, protein was transferred to a PVDF membrane and blocked with 5% bovine serum albumin or skim milk in Tris-buffered saline containing 0.1% Tween 20 for 1.5 h. Membranes were incubated overnight with primary antibodies AT1R, PLCβ, CREB, or β-actin. Secondary antibodies were incubated for 2 h, and the blotted membranes were prepared with ECL substrate (Thermo Scientific). Band intensities were quantified by densitometry.

Statistical analysis

All the experimental data were presented as mean + SD. $P < 0.05$ was considered as statistically significant. SPSS (version 20.0) software was used for statistical analyses. Two-way repeated measure ANOVA by Bonferroni's post hoc multiple-comparisons test was used to examine the effect of 5CAN and 10CAN on SA performance maintained by different doses of METH. One-way ANOVA was used to examine the effect 5CAN and 10CAN on cue- and drug-induced reinstatement of METH SA. Western blot data were expressed as a ratio of D2R/β-actin and AT1R/β-actin. One-way ANVOA was applied to examine the changes of D2R/β-actin and AT1R/β-actin in different brain regions. Independent t-test was used to compare the changes of miR-219a-5p expression among yoked-saline, yoked-METH, and METH SA groups. Two-way repeated measure ANOVA with Bonferroni's *post hoc*

JPET Fast Forward. Published on March 13, 2019 as DOI: 10.1124/jpet.118.255729
This article has not been copyedited and formatted. The final version may differ from this version.

multiple-comparisons test was used to study the effects of miR-219a-5p overexpression on SA performance maintained by different doses of METH. Independent t-test was used to analyze the changes of miR-219-5p expression between LV1NC and LV1-miR-219a-5p groups. Independent t-test was also used to study the effects of miR-219-5p overexpression on cue- or drug-induced reinstatement of METH SA and the expression of miR-219-5p of LV1NC vs. LV1-miR-219-59. Western blot and qPCR data were expressed as a ratio of AT1R/ PLCβ/ CREB. These data were analyzed by an independent t-test between groups.

Results

The effect of AT1R blockade on METH SA and cue-/drug- induced reinstatement

The effects of CAN on METH SA and cue-/drug-induced reinstatement are shown in Fig 1. There was a major effect of Group ($F_{(3,89)}$=68.819, p<0.001, Fig 1A), Dose ($F_{(3,89)}$=28.036, p<0.001, Fig 1A) and Group X Dose interaction ($F_{(6,89)}$=48.427, p<0.001, Fig 1A). Under the FR1 schedule, increasing the dose of METH significantly decreased METH SA for all four groups. Compared with Saline+METH, DMSO+METH and 5CAN+METH rats, 10CAN+METH rats earned significantly fewer infusions of 0.025 and 0.05 mg/kg/infusion METH under the FR1 schedule (p<0.01, Fig 1A). However, there was no major effect of CAN on the two highest does of METH (p>0.05, Fig 1A). Neither 5 and 10 CAN produced significant effects on inactive nose-poke responses during the period of METH SA under FR1 schedule (Supplemental Figure 1). The effect of CAN on METH SA under the PR schedule is

JPET Fast Forward. Published on March 13, 2019 as DOI: 10.1124/jpet.118.255729
This article has not been copyedited and formatted. The final version may differ from this version.

shown in Fig 1B. There was a major effect of Group ($F_{(3,89)}$ =36.394, p <0.01, Fig 1B), Dose ($F_{(3,89)}$ =19.502, p <0.01, Fig 1B) and Group X Dose interaction ($F_{(6,89)}$ = 27.947, p <0.01, Fig 1B). Increasing the dose of METH produced a significant increase in the breakpoints for all four groups. Further *post hoc* analysis indicated that the Saline+METH and DMSO+METH rats produced significantly higher breakpoints maintained by 0.075 mg/kg/infusion of METH than those of the 5CAN+METH (p <0.05, Fig 1B) and 10CAN+METH (p <0.01, Fig 1B) rats. In addition, 10CAN+METH rats produced significantly fewer breakpoints maintained by 0.1 mg/kg/infusion of METH than those of the Saline+METH, DMSO+METH and 5CAN+METH rats (p<0.01, Fig 1B). Fig 1C illustrates the effect of CAN on the cue-induced reinstatement of METH SA. Compared with the Saline and DMSO groups, the responses significantly decreased in the 5CAN (p <0.05, Fig 1C) and 10CAN (p <0.01, Fig 1C) groups. Relative to 5CAN, 10CAN produced significantly fewer responses (p <0.05, Fig 1C). The effect of CAN on drug-induced reinstatement is shown in Fig 1D. The responses significantly decreased in the 5CAN (p<0.05, Fig 1D) and 10CAN (p<0.01, Fig 1D) groups, compared with those of the Saline and DMSO groups. Relative to 5CAN, 10CAN produced significantly fewer responses (p<0.01, Fig 1D). The animals among all groups did not show significant differences in responses on inactive poke (p>0.05, Fig 1D).

Expression of D2R and AT1R in various brain regions of METH SA rats treated with CAN

The effect of CAN on the expression of D2R and AT1R in METH SA rats is shown in Fig 2. One-way ANOVA analysis showed a significant effect of Group on the level of D2R/β-actin in VTA ($F_{(2,8)}$=87.111, p<0.01, Fig 2A), NAc ($F_{(2,8)}$=34.901, p <0.01, Fig 2A) and PFC ($F_{(2,8)}$=75.434, p<0.01, Fig 2A) of rats self-administering METH maintained by FR1 schedule. The major effect of Group was not shown in Hip and CPU. Further *post hoc* analysis revealed that D2R/β-actin level of group 10CAN+METH was significantly lower than that of group DMSO+METH and 5CAN+METH in VTA, NAc and PFC (p<0.05, Fig 2A). There were no significant differences in D2R/β-actin expression between DMSO+METH and 5CAN+METH groups across all tested brain regions (p>0.05, Fig 2A). One-way ANOVA revealed that there was a significant effect of Group on the expression of AT1R/β-actin in VTA ($F_{(2,8)}$=29.621, p<0.01, Fig 2B), NAc ($F_{(2,8)}$=52.215, p <0.01, Fig 2B) and PFC ($F_{(2,8)}$=43.583, p<0.01, Fig 2B) of rats self-administering METH maintained by FR1 schedule. Such an effect was not evident in Hip and CPU. Further *post hoc* analysis revealed that VTA and PFC AT1R/β-actin level of group 10CAN+METH was significantly lower that of group DMSO+METH and 5CAN+METH groups (p<0.01, Fig 2B). In NAc, AT1R/β-actin level of group 10CAN+METH was significantly lower that of group DMSO+METH (p<0.01, Fig 2B). There was also a significant difference AT1R/β-actin level between group METH+5CAN and DMSO+METH in NAc (p<0.05, Fig 2B).

A one-way ANOVA analysis showed a major effect of Group on D2R/β-actin level in

Hip ($F_{(2,8)}$ =15.375, p<0.01, Fig 2D) and NAc ($F_{(2,8)}$ =3.314, p<0.05, Fig 2D) of rats self-administering METH maintained by PR schedule. D2R/β-actin level was not significantly different among groups in the brain regions of VTA, PFC and CPU. Further *post hoc* test showed that Hip and NAc D2R/β-actin level in 10CAN+METH rats was significantly lower than that in DMSO+METH and 5CAN+METH groups (p<0.01, Fig 2D). There was a significant effect of Group in AT1R/β-actin expression in VTA ($F_{(2,8)}$ =65.979, p<0.01, Fig 2E) and NAc ($F_{(2,8)}$ =21.132, p<0.01, Fig 2E). Such an effect was not observed in Hip, PFC and CPU. Further *post hoc* test showed that both VTA and NAc, AT1R/β-actin in group 10CAN+METH was significantly lower than that in group DMSO+METH and 5CAN+METH (p<0.01, Fig 2E).

Expression of D2R and AT1R in various brain regions of rats treated with CAN following cue- and drug-induced reinstatement of METH SA

The effect of CAN on the expression of D2R and AT1R in METH following cue- and drug-induced reinstatement of METH SA was presented in Fig 3. There was a major effect of Group on D2R/β-actin level in VTA ($F_{(3,15)}$ =15.321, p<0.01, Fig 3A), NAc ($F_{(3,15)}$ =53.313, p<0.01, Fig 3A) and PFC ($F_{(3,15)}$ =18.926, p<0.01, Fig 3A) in rats with cue-induced reinstatement of METH SA. D2R/β-actin level was not significantly different among groups in Hip and CPU. Further *post hoc* test showed that VTA, NAc and PFC D2R/β-actin level in 10CAN+METH rats was significantly lower than that in DMSO+METH groups (p<0.01, Fig 3A). There was a significant effect of Group in the expression of AT1R/β-actin in Hip ($F_{(3,15)}$ =34.231, p<0.01, Fig 3-A2), VTA ($F_{(3,15)}$

=6.534, p<0.01, Fig 3B), NAc ($F_{(3,15)}$ = 11.42, p < 0.01, Fig 3B) and PFC ($F_{(3,15)}$ = 6.321, p < 0.01, Fig 3B). Such an effect was not observed in CPU. Further *post hoc* test showed that in Hip, VTA, NAc and PFC, AT1R/β-actin in group 10CAN+METH was significantly lower than that in DMSO+METH group (p<0.01, Fig 3B).

A one-way ANOVA analysis showed a major effect of Group on D2R/β-actin level in VTA ($F_{(3,15)}$ =4.921, p<0.01, Fig 3D), NAc ($F_{(3,15)}$ =3.343, p<0.01, Fig 3D) and PFC ($F_{(3,15)}$ =14.956, p<0.01, Fig 3D) of rats with drug-induced reinstatement of METH SA. D2R/β-actin level was not significantly different among groups in Hip and CPU. Further *post hoc* test showed that VTA, NAc and PFC D2R/β-actin level in saline SA rats was significantly lower than that in METH SA rats (p<0.05, Fig 3D). VTA, NAc and PFC D2R/β-actin level in group 10CAN was also significantly lower than that in group DMSO (p<0.05, Fig 3D). There was a significant effect of Group in the expression of AT1R/β-actin in Hip ($F_{(3,15)}$ =34.231, p<0.01, Fig 3E), VTA ($F_{(3,15)}$ =6.534, p <0.01, Fig 3E), NAc ($F_{(3,15)}$ = 11.42, p<0.01, Fig 3E) and PFC ($F_{(3, 15)}$ = 6.321, p<0.01, Fig 3E). Such an effect was not observed in CPU. Further *post hoc* test showed that Hip, VTA, NAc and PFC AT1R/β-actin level in saline SA rats was significantly lower than that in METH SA rats (p<0.05, Fig 3E). Hip, VTA, NAc and PFC AT1R/β-actin level in group 10CAN was also significantly lower than that in group DMSO (p<0.05, Fig 3E).

The effect of METH SA on miRNA expression targeting AT1R

The effects of METH SA on miRNAs are shown in Fig 4. METH SA rats received an

average of 87 infusions during the maintenance period of METH SA (Fig 4A). Up-regulated and down-regulated miRNAs were identified in yoked-Saline group, yoked-METH group and METH SA group (Fig 4B). Colors in the heat map indicate the correlation between the different data sets. The intersection of the data was calculated by Venn diagrams and shown by heatmap. As shown in Fig 4C, a total 17 miRNAs associated with RAS were significantly changed in the NAc of METH SA rats, compared with yoked-METH and yoked-saline rats (fold change $\geqslant$1.5, p< 0.05). A total of 8 miRNAs levels were up-regulated; whereas 9 miRNAs levels were down-regulated following METH SA. Compared with the yoked-METH and yoked-saline rats, miR-219a-5p was downregulated by 3.04-fold and 5.43-fold respectively in the NAc of METH SA rats (Fig 4D). As shown in Fig 4E, further independent t-test analysis revealed that the levels of miR-219a-5p were significantly down-regulated in the NAc of METH SA rats, compared with yoked-METH and yoked-saline rats (Yoked-METH vs METH SA, p<0.001; Yoked-saline vs METH SA, p<0.001).

The effect of miR-219a-5p overexpression in the NAc on METH SA under the FR1 and PR schedule

Fig 5A illustrates the effects of miR-219a-5p overexpression in the NAc on METH SA under the FR1 schedule. There was a significant effect of Group ($F_{(2,83)}$ =18.071, p<0.001), Dose ($F_{(3,83)}$ =265.736, p<0.001), and a Group X Dose interaction ($F_{(6,83)}$ =0.618, p=0.715). Increasing the dose of METH produced a significant decrease in

METH consumption for all four groups. *Post hoc* analysis indicated that the LV1-miR-219a-5p group earned significantly fewer infusions of 0.05, 0.075 and 0.1 mg/kg/infusion of METH than Baseline and LV1NC group (0.05 mg/kg/infusion METH/LV1NC vs. LV1-miR-219a-5p: $p<0.01$; 0.05 mg/kg/infusion METH/Baseline vs. LV1-miR-219a-5p: $p<0.001$; 0.075 mg/kg/infusion/METH: LV1NC vs. LV1-miR-219a-5p: $p<0.001$; 0.075 mg/kg/infusion METH/Baseline vs. LV1-miR-219a-5p: $p<0.01$; 0.1 mg/kg/infusion/METH: LV1NC vs. LV1-miR-219a-5p: $p<0.001$; 0.1 mg/kg/infusion METH/Baseline vs. LV1-miR-219a-5p: $p<0.05$). However, the differences for 0.025 mg/kg/infusion of METH failed to reach significance among three groups ($p>0.05$, Fig 5A). As shown in Fig 5B, the expression of NAc miR-219a-5p of the LV1-219a-5p group under the FR1 schedule was significantly higher than that of the LV1NC group ($p<0.05$).

The effects of NAc miR-219a-5p overexpression on METH SA under the PR schedule are shown in the Fig 5C. There was a significant effect of Group ($F_{(3,54)}=49.488$, $p<0.001$); Dose ($F_{(2,54)}=107.095$, $p<0.001$), and a Group X Dose interaction ($F_{(6,54)}=15.390$, $p<0.001$). Increasing the dose of METH produced a significant increase in the breakpoints for all four groups. Further *post hoc* analysis indicated that Baseline and LV1NC group produced significantly higher breakpoints maintained by 0.05, 0.075 and 0.1 mg/kg/infusion of METH than those of the LV1-miR219a-5p group (0.05 mg/kg/infusion METH/LV1NC vs. LV1-miR-219a-5p, $p<0.001$; 0.05 mg/kg/infusion METH/Baseline vs. LV1-miR-219a-5p, $p<0.001$; 0.075 mg/kg/infusion METH/LV1NC

JPET Fast Forward. Published on March 13, 2019 as DOI: 10.1124/jpet.118.255729
This article has not been copyedited and formatted. The final version may differ from this version.

vs. LV1-miR-219a-5p, $p<0.001$; 0.075 mg/kg/infusion METH/Baseline vs. LV1-miR-219a-5p, $p<0.001$; 0.1 mg/kg//infusion METH/LV1NC vs. LV1-miR-219a-5p, $p<0.001$; 0.1mg/kg//infusion METH/Baseline vs. LV1-miR-219a-5p, ($p<0.001$). No differences were identified for the 0.025 mg/kg/infusion of METH ($p>0.05$). As shown in Fig 5D, the expression of NAc miR-219a-5p in LV1-219a-5p group was significantly higher than that in the LV1NC group under the PR schedule ($p<0.001$).

The effect of miR-219a-5p overexpression on cue- and drug-induced reinstatement of METH SA in NAc

The effect of miR-219a-5p overexpression in NAc on cue-induced reinstatement is shown in Fig 6A. The independent sample t-test analysis showed that the LV1NC rats exhibited significantly more responses than those of the LV1-miR-219a-5p rats ($p<0.01$). As shown in Fig 6B for the cue-induced reinstatement of METH SA, the expression of NAc miR-219a-5p of the LV1-219a-5p rats was significantly higher than that in the LV1NC rats ($p<0.001$). The effect of miR-219a-5p overexpression in NAc on the drug-induced reinstatement of METH SA is shown in Fig 6C. The independent t-test analysis showed that the LV1-miR-219a-5p rats exhibited significantly fewer responses than those of the LV1NC rats ($p<0.01$). As shown in Fig 6D for the drug-induced reinstatement of METH SA, the expression of NAc miR-219a-5p in the LV1-219a-5p group was significantly higher than that in the LV1NC group ($p<0.001$). Following the micro-injection, the injection site of NAc for each animal was examined

JPET Fast Forward. Published on March 13, 2019 as DOI: 10.1124/jpet.118.255729
This article has not been copyedited and formatted. The final version may differ from this version.

by a fluorescence microscope (Supplemental Figure 1).

The changes of AT1R, PLCβ and CREB expression in METH SA rats with miR-219a-5p overexpression

Fig 7 illustrates the expression of AT1R, PLCβ and CREB proteins in LV1NC and LV1-miR-219a-5p groups, following METH SA and cue-/drug-induced reinstatement. The levels of AT1R, PLCβ and CREB were significantly decreased in the LV1-miR-219a-5p rats self-administering METH under the FR1 schedule, compared with the LV1NC rats (p<0.05, Fig 7A). METH SA under the PR schedule and cue- and drug-induced reinstatement showed similar trends, as shown in Fig 7B, 7C and 7D respectively (p<0.05).

The expression of AT1R, PLCβ and CREB in PC12 cells using western blotting was shown in Fig 8. The expression of AT1R were increased significantly in the 2.0mM METH group and was markedly attenuated in 2.5, 5.0, 10.0, and 20.0 μM CAN groups (p<0.001; Fig 8B). Similarly, the level of PLCβ and CREB were also increased significantly in the 2.0mM METH group and decreased following the treatment of 2.5, 5.0, 10.0, and 20.0 μM CAN in PC12 cells (p<0.001; Fig 8C and 8D). Fig 8E-G shows the mRNA levels of Agtr1b, PLCβ1 and CREB1 in PC12 cells. In the control PC12 cells, the mRNA levels measured by RT-qPCR were normalized by the β-actin miRNA levels and set as 1. The treatment of 2.0 mM METH significantly increased the levels of Agtr1b, PLCβ1and CREB1 mRNA (p<0.001, Fig 8E, 8F and 8G). The increased

levels of Agtr1b, PLCβ1and CREB1 mRNA induced by 2.0 mM METH were significantly decreased by the treatment of 2.5, 5.0, 10.0, and 20.0 μM CAN (p<0.001, Fig 8E, 8F and 8G).

Discussion

The present study demonstrated that AT1R blockade by CAN significantly reduced METH SA and cue-/drug-induced reinstatement in a dose-dependent manner, in conjunction with altered D2R level. Involuntary intake of METH also led to a significant decrease in a total of 17 miRNAs targeting Ang and AT1R in NAc. The overexpression of NAc miR-219a-5p targeting AT1R significantly decreased METH SA under the FR1/PR schedule and cue-/drug-induced reinstatement via the AT1R-PLCβ-CREB signaling pathway. Finally, our findings suggest that different subtypes of PLCβ may play a distinctive role in the modulation of METH effects by AT1R blockade.

The present studies also demonstrated that the inhibition of AT1R by CAN at the dose of 10 mg/kg reduced both METH SA under the FR/PR schedule and cue-/drug-induced reinstatement. Treatment of 10 mg/kg CAN substantially reduced the elevated D2R expression induced by METH SA and reinstatement mainly in the NAc and PFC. Excess release of dopamine and dysregulation of the central dopaminergic system have largely been suggested to be responsible for the behavioral outcomes of METH (Ares-Santos et al., 2013; Courtney and Ray, 2014; Jablonski et al., 2016).

JPET Fast Forward. Published on March 13, 2019 as DOI: 10.1124/jpet.118.255729
This article has not been copyedited and formatted. The final version may differ from this version.

Antagonistic interactions between the dopaminergic system and AT1R blockade have been described in the rat striatum and substantia nigra (Dominguez-Meijide et al., 2014). Overactivation of RAS has been shown to induce dopamine depletion, which could be prevented by AT1R blockers and angiotensin-converting enzyme inhibitors (Labandeira-Garcia et al., 2013). Overexpression of AT1R in the striatum and substantia nigra was evident in D2R-deficient mice and rats (Villar-Cheda et al., 2010). This counterregulator effect could be explained by the functional heteromers formed by AT1R and D2R in the striatum, which was confirmed by in situ proximity ligation assay labeling (Martinez-Pinilla et al., 2015). It is unlikely that the decrease in METH SA was due to the nonspecific effects of AT1R blockade on the motor effect of METH. We examined the effects of 5 and 10 mg/kg CAN on the locomotor activity of METH. Neither the treatment of 5 nor 10 mg/kg CAN significantly affected the locomotor activity of METH (unpublished data). CAN is the prodrug of candesartan. Other studies have also demonstrated that administration of candesartan did not significantly alter the locomotor activity of rats (Gaur and Kumar, 2011). Furthermore, candersartan has been shown to improve motor dysfunction induced by stroke and thioacetamide-induced chronic liver failure in rats (Gaur and Kumar, 2011; Murad et al., 2017). As mentioned previously, an increasing number of studies have highlighted the potential use of medications targeting cognitive impairments associated with executive function for METH use disorder (Sofuoglu et al., 2013).

The current study demonstrated the downregulation of NAc miR-219p-5p targeting

AT1R following METH SA, compared with yoked METH and saline rats. current findings extend the increasing bodies of research that have demonstrated METH enabled alterations in a number of NAc miRNA expressions associated with various neuronal activities, including metabolism, apoptosis, autophagy and the immune response, potentially via the MAPK, CREB, G-Protein Coupled Receptor and GnRH signaling pathways (Zhu et al., 2015; Bai et al., 2016; Sim et al., 2017; Li et al., 2018; Zhang et al., 2018). A clinical study has also identified numerous miRNAs as negative regulators in patients with METH use disorder. The majority of studies have used the model of locomotor sensitization and conditioned place preference induced by METH that involves repeated passive administration of METH (Zhu et al., 2015; Li et al., 2018). Two recent studies have investigated the changes of miRNA in rats self-administering METH. In both studies, control animals SA saline upon active responses (Bosch et al., 2015; Du et al., 2016). Twenty-eight miRNAs in the prefrontal cortex and VTA were identified in rats with short and long access to METH SA, compared with animals trained to SA saline (Du et al., 2016). Seventy-eight miRNAs were differentially expressed in rats self-administering METH, compared with saline control animals (Bosch et al., 2015). The present study identified 107 NAc miRNAs related to METH self-seeking behavior by comparing METH SA and METH-yoked rats. We further identified 17 miRNAs that targeted brain RAS among which 3, 5, and 9 miRNAs are associated with AngII, Agtr1a and Agtr1b, respectively. To further investigate the altered activities of miRNAs that modulate METH SA, the effects of the overexpression of miR-219a-5p targeting AT1R were investigated with the animal

model of METH SA under the FR/PR schedule and cue-/drug-induced reinstatement. MiR-219a-5p was selected because it produced the most significant p-values and fold change in METH SA rats compared with the yoked METH and yoked Saline rats. FR and PR schedules have commonly been used to investigate the reinforcing and motivation effects of drugs of abuse (Killeen et al., 2009; Poling, 2010). The overexpression of miR-219a-5p in NAc significantly decreased METH SA at the three highest tested doses of METH under the FR and PR schedules. The potential effect of altered miR-219a-5p on cue- and drug-induced reinstatement of METH SA was subsequently examined. Similarly, the overexpression of miR-219a-5p in NAc significantly reduced the responses during both cue- and drug-induced reinstatement of METH SA tests.

The current study showed that the effect of AT1R on the behavioral effects of METH was associated with the changes of CREB and PLCβ, along with the altered activity of D2R. There has been growing evidence about the interaction between D2R and PLC. PLC antagonist, U-73122, has been demonstrated to inhibit the effect of D2R activation by Quinpirole on GABAergic neurons (Jijon-Lorenzo et al., 2018). Reduced inositol triphosphate 1(IP1) level, which indicated lower activity of PLC, was evident in cells with D2R knockdown(Simanjuntak et al., 2017). Motor skill learning deficits induced by D2R antagonists, raclopride, were prevented by coadministration of the PLC agonist, m-3m3fbs (Rioult-Pedotti et al., 2015). Furthermore, the activation of PLC has also been suggested to modulate the suppressive effects of D2R stimulation

on transmembrane Ca2+ currents in enkephalin-expressing medium spiny neurons(Hernandez-Lopez et al., 2000). PLC blockade by U-73122 inhibited diethylstilbestrol-induced Ca2+ mobilization and activation of CREB in gubernaculum testis cells, which suggests the underlying PLC-Ca2+ -CREB pathway (Zhang et al., 2018). Orexin-A dose-dependently increased Ca2+ in dopamine-containing neurons, which could be abolished by a phosphatidylcholine-specific PLC inhibitor, D609 (Uramura et al., 2001). It is likely PLC regulates the effects of AT1R on METH through the changes of D2R and CREB/Ca2+ could the important regulator in this process(Hamilton et al., 2015; Hille et al., 2015). PLC are classified into six isotypes, including β, γ, δ, ε, ζ, and η. PLCβ is one of the most extensively studied PLCs. Due to the lack of selective antagonist of the isotypes of PLC, it remains unknown how the specific isotypes of PLC is involved in the process. The current studies have demonstrated that the activity of PLCβ was significantly altered, in conjunction with the changes of AT1R and CREB. It is proposed that the activation of AT1R results the cleavage of inositol triphosphate 3 (IP3) and diacylglycerol (DAG) from PLC. IP3 increases the flow of Ca^{2+} from the Endoplasmic Reticulum (ER) and increases the concentration of Ca^{2+}. DAG activates protein kinase C (PKC), which subsequently activates CREB via phosphorylation (Liu et al., 2002; Song et al., 2011; Kuraishi et al., 2013; Oubrahim et al., 2013). Figure 9 illustrates the proposed link among AT1R, PLCβ and CREB.

The primary PLC isozymes PLCβ1 and PLCβ4 are highly expressed and differentially

distributed in the brain, which suggests a specific role for each PLC subtype in different regions of the brain (Yang et al., 2016). PLCβ1 is detected at high levels in the cerebral cortex, hippocampus, amygdala, lateral septum, and olfactory bulb (Ross et al., 1989). Disruption of PLCβ1-mediated signaling in the brain has also been suggested to be the underlying mechanism of epilepsy, schizophrenia, and bipolar disorder (Kim et al., 1997; Garcia del Cano et al., 2014). PLCβ4 is expressed at high levels in the retina and cerebellum; however, it is rarely detected in the forebrain (Tanaka and Kondo, 1994). Dysfunction of PLCβ4 is thought to be associated with ataxia, absence seizures, and visual processing defects(Cheong et al., 2009). Furthermore, abnormal expression of PLCβ4 was identified in individuals with Huntington's disease (Cheong et al., 2009). In Experiment 4, we specifically investigated the changes of PLCβ1 and PLCβ4 in cells following the co-administration of METH and CAN. The co-administration of CAN dose-dependently prevented the increased levels of PLCβ1 and PLCβ4 by METH. It is noted that both PLCβ1 and PLCβ4 seem to involve the regulatory role of AT1R in METH effects. As previously discussed, METH use disorder shares common symptoms and mechanisms with a wide range of mental disorders. It is not surprising that both PLCβ1 and PLCβ4, which undermine different categories of mental disorders, are involved in METH effects.

In conclusion, the present study indicates that AT1R plays an important role in METH SA and cue-/drug-induced reinstatement of METH SA, which may provide an entirely new direction for the development of pharmacotherapeutics for METH use disorder.

Acknowledgements

Dr. Huifen Liu provided assistance.

Authorship Contributions

Participated in research design: Liu, Cui, Xu (Huachong), Zhou

Conducted experiments: Xu (Xing), Pan, Li (Xingxing), and Wu

Performed data analysis: Mao, Xu (Huachong), Mao

Wrote or contributed to the writing of the manuscript: Liu, Pan, Xu (Xing)

References

Ares-Santos S, Granado N and Moratalla R (2013) The role of dopamine receptors in the neurotoxicity of methamphetamine. *J Intern Med* **273**:437-453.

Bai Y, Zhang Y, Hua J, Yang X, Zhang X, Duan M, Zhu X, Huang W, Chao J, Zhou R, Hu G and Yao H (2016) Silencing microRNA-143 protects the integrity of the blood-brain barrier: implications for methamphetamine abuse. *Sci Rep* **6**:35642.

Basmadjian OM, Occhieppo VB, Marchese NA, Baiardi G and Bregonzio C (2017) Brain Angiotensin II Involvement in Chronic Mental Disorders. *Protein Pept Lett* **24**:817-826.

Bernheim A, See RE and Reichel CM (2016) Chronic methamphetamine self-administration disrupts cortical control of cognition. *Neurosci Biobehav Rev* **69**:36-48.

Bosch PJ, Benton MC, Macartney-Coxson D and Kivell BM (2015) mRNA and microRNA analysis reveals modulation of biochemical pathways related to addiction in the ventral tegmental area of methamphetamine self-administering rats. *BMC Neurosci* **16**:43.

Cami J and Farre M (2003) Drug addiction. *N Engl J Med* **349**:975-986.

Casarsa BS, Marinzalda MA, Marchese NA, Paz MC, Vivas L, Baiardi G and Bregonzio C (2015) A previous history of repeated amphetamine exposure modifies brain angiotensin II AT1 receptor functionality. *Neuroscience* **307**:1-13.

Cheong E, Zheng Y, Lee K, Lee J, Kim S, Sanati M, Lee S, Kim YS and Shin HS (2009) Deletion of phospholipase C beta4 in thalamocortical relay nucleus leads to absence seizures. *Proc Natl Acad Sci U S A* **106**:21912-21917.

Courtney KE and Ray LA (2014) Methamphetamine: an update on epidemiology, pharmacology, clinical phenomenology, and treatment literature. *Drug Alcohol Depend* **143**:11-21.

Dominguez-Meijide A, Villar-Cheda B, Garrido-Gil P, Sierrra-Paredes G, Guerra MJ and Labandeira-Garcia JL (2014) Effect of chronic treatment with angiotensin type 1 receptor antagonists on striatal dopamine levels in normal rats and in a rat model of Parkinson's disease treated with L-DOPA. *Neuropharmacology* **76 Pt A**:156-168.

Du HY, Cao DN, Chen Y, Wang L, Wu N and Li J (2016) Alterations of prefrontal cortical microRNAs in methamphetamine self-administering rats: From controlled drug intake to escalated drug intake. *Neurosci Lett* **611**:21-27.

Erlandson KM, Kitch D, Wester CW, Kalayjian RC, Overton ET, Castillo-Mancilla J, Koletar SL, Benson CA, Campbell TB, Robertson K and Lok JJ (2017) The Impact of Statin and Angiotensin-Converting Enzyme Inhibitor/Angiotensin Receptor Blocker Therapy on Cognitive Function in Adults With Human Immunodeficiency Virus Infection. *Clin Infect Dis* **65**:2042-2049.

Fan X, Song X, Zhao M, Jarskog LF, Natarajan R, Shukair N, Freudenreich O, Henderson DC and Goff DC (2017) The effect of adjunctive telmisartan treatment on psychopathology and cognition in patients with schizophrenia. *Acta Psychiatr Scand* **136**:465-472.

Franke AG, Bagusat C, Rust S, Engel A and Lieb K (2014) Substances used and prevalence rates of pharmacological cognitive enhancement among healthy subjects. *Eur Arch Psychiatry Clin Neurosci* **264 Suppl 1**:S83-90.

Fulcher JA, Hussain SK, Cook R, Li F, Tobin NH, Ragsdale A, Shoptaw S, Gorbach PM and Aldrovandi GM (2018) Effects of Substance Use and Sex Practices on the Intestinal Microbiome During HIV-1 Infection. *J Infect Dis*.

Gao J, Xu Z, Li X, O'Brien JW, Culshaw PN, Thomas KV, Tscharke BJ, Mueller JF and Thai PK (2018)

Enantiomeric profiling of amphetamine and methamphetamine in wastewater: A 7-year study in regional and urban Queensland, Australia. *Sci Total Environ* **643**:827-834.

Garcia del Cano G, Montana M, Aretxabala X, Gonzalez-Burguera I, Lopez de Jesus M, Barrondo S and Salles J (2014) Nuclear phospholipase C-beta1 and diacylglycerol LIPASE-alpha in brain cortical neurons. *Adv Biol Regul* **54**:12-23.

Gaur V and Kumar A (2011) Neuroprotective potentials of candesartan, atorvastatin and their combination against stroke induced motor dysfunction. *Inflammopharmacology* **19**:205-214.

Grant KM, LeVan TD, Wells SM, Li M, Stoltenberg SF, Gendelman HE, Carlo G and Bevins RA (2012) Methamphetamine-associated psychosis. *J Neuroimmune Pharmacol* **7**:113-139.

Hamilton A, Zamponi GW and Ferguson SS (2015) Glutamate receptors function as scaffolds for the regulation of beta-amyloid and cellular prion protein signaling complexes. *Mol Brain* **8**:18.

Hartel-Petri R, Krampe-Scheidler A, Braunwarth WD, Havemann-Reinecke U, Jeschke P, Looser W, Muhlig S, Schafer I, Scherbaum N, Bothe L, Schaefer C and Hamdorf W (2017) Evidence-Based Guidelines for the Pharmacologic Management of Methamphetamine Dependence, Relapse Prevention, Chronic Methamphetamine-Related, and Comorbid Psychiatric Disorders in Post-Acute Settings. *Pharmacopsychiatry* **50**:96-104.

Hernandez-Lopez S, Tkatch T, Perez-Garci E, Galarraga E, Bargas J, Hamm H and Surmeier DJ (2000) D2 dopamine receptors in striatal medium spiny neurons reduce L-type Ca2+ currents and excitability via a novel PLC[beta]1-IP3-calcineurin-signaling cascade. *The Journal of neuroscience : the official journal of the Society for Neuroscience* **20**:8987-8995.

Hille B, Dickson EJ, Kruse M, Vivas O and Suh BC (2015) Phosphoinositides regulate ion channels. *Biochimica et biophysica acta* **1851**:844-856.

Holme MN, Rashid MH, Thomas MR, Barriga HMG, Herpoldt KL, Heenan RK, Dreiss CA, Banuelos JL, Xie HN, Yarovsky I and Stevens MM (2018) Fate of Liposomes in the Presence of Phospholipase C and D: From Atomic to Supramolecular Lipid Arrangement. *ACS Cent Sci* **4**:1023-1030.

Hosseini M, Alaei HA, Havakhah S, Neemati Karimooy HA and Gholamnezhad Z (2009) Effects of microinjection of angiotensin II and captopril to VTA on morphine self-administration in rats. *Acta Biol Hung* **60**:241-252.

Hosseini M, Sharifi MR, Alaei H, Shafei MN and Karimooy HA (2007) Effects of angiotensin II and captopril on rewarding properties of morphine. *Indian J Exp Biol* **45**:770-777.

Im HI, Hollander JA, Bali P and Kenny PJ (2010) MeCP2 controls BDNF expression and cocaine intake through homeostatic interactions with microRNA-212. *Nat Neurosci* **13**:1120-U1121.

Jablonski SA, Williams MT and Vorhees CV (2016) Mechanisms involved in the neurotoxic and cognitive effects of developmental methamphetamine exposure. *Birth Defects Res C Embryo Today* **108**:131-141.

Jiang L, Zhu R, Bu Q, Li Y, Shao X, Gu H, Kong J, Luo L, Long H, Guo W, Tian J, Zhao Y and Cen X (2018) Brain Renin-Angiotensin System Blockade Attenuates Methamphetamine-Induced Hyperlocomotion and Neurotoxicity. *Neurotherapeutics* **15**:500-510.

Jijon-Lorenzo R, Caballero-Floran IH, Recillas-Morales S, Cortes H, Avalos-Fuentes JA, Paz-Bermudez FJ, Erlij D and Floran B (2018) Presynaptic Dopamine D2 Receptors Modulate [(3)H]GABA Release at StriatoPallidal Terminals via Activation of PLC-->IP3-->Calcineurin and Inhibition of AC-->cAMP-->PKA Signaling Cascades. *Neuroscience* **372**:74-86.

Killeen PR, Posadas-Sanchez D, Johansen EB and Thrailkill EA (2009) Progressive ratio schedules of reinforcement. *J Exp Psychol Anim Behav Process* **35**:35-50.

Kim D, Jun KS, Lee SB, Kang NG, Min DS, Kim YH, Ryu SH, Suh PG and Shin HS (1997) Phospholipase C isozymes selectively couple to specific neurotransmitter receptors. *Nature* **389**:290-293.

Knuepfer MM, Rowe KD, Schwartz JA and Lomax LL (2005) Role of angiotensin II and corticotropin-releasing hormone in hemodynamic responses to cocaine and stress. *Regul Pept* **127**:1-10.

Krizman-Matasic I, Senta I, Kostanjevecki P, Ahel M and Terzic S (2018) Long-term monitoring of drug consumption patterns in a large-sized European city using wastewater-based epidemiology: Comparison of two sampling schemes for the assessment of multiannual trends. *Sci Total Environ* **647**:474-485.

Kuraishi T, Hori A and Kurata S (2013) Host-microbe interactions in the gut of Drosophila melanogaster. *Front Physiol* **4**:375.

Labandeira-Garcia JL, Rodriguez-Pallares J, Dominguez-Meijide A, Valenzuela R, Villar-Cheda B and Rodriguez-Perez AI (2013) Dopamine-angiotensin interactions in the basal ganglia and their relevance for Parkinson's disease. *Mov Disord* **28**:1337-1342.

Li H, Li C, Zhou Y, Luo C, Ou J, Li J and Mo Z (2018) Expression of microRNAs in the serum exosomes of methamphetamine-dependent rats vs. ketamine-dependent rats. *Exp Ther Med* **15**:3369-3375.

Li H, Wang Y, Wang Z, Guo X, Wang F, Xia XJ, Zhou J, Shi K, Yu JQ and Zhou YH (2016) Microarray and genetic analysis reveals that csa-miR159b plays a critical role in abscisic acid-mediated heat tolerance in grafted cucumber plants. *Plant Cell Environ* **39**:1790-1804.

Liu F, Virshup DM, Nairn AC and Greengard P (2002) Mechanism of regulation of casein kinase I activity by group I metabotropic glutamate receptors. *The Journal of biological chemistry* **277**:45393-45399.

Martinez-Pinilla E, Rodriguez-Perez AI, Navarro G, Aguinaga D, Moreno E, Lanciego JL, Labandeira-Garcia JL and Franco R (2015) Dopamine D2 and angiotensin II type 1 receptors form functional heteromers in rat striatum. *Biochem Pharmacol* **96**:131-142.

McKetin R, Lubman DI, Baker AL, Dawe S and Ali RL (2013) Dose-related psychotic symptoms in chronic methamphetamine users: evidence from a prospective longitudinal study. *JAMA Psychiatry* **70**:319-324.

Mullen JM and Crawford AT (2018) Amphetamine Related Psychiatric Disorders, in *StatPearls*, Treasure Island (FL).

Murad HA, Gazzaz ZJ, Ali SS and Ibraheem MS (2017) Candesartan, rather than losartan, improves motor dysfunction in thioacetamide-induced chronic liver failure in rats. *Braz J Med Biol Res* **50**:e6665.

Muthuraman A and Kaur P (2016) Renin-Angiotensin-Aldosterone System: A Current Drug

Target for the Management of Neuropathic Pain. *Curr Drug Targets* **17**:178-195.

Oubrahim H, Wong A, Wilson BA and Chock PB (2013) Mammalian target of rapamycin complex 1 (mTORC1) plays a role in Pasteurella multocida toxin (PMT)-induced protein synthesis and proliferation in Swiss 3T3 cells. *The Journal of biological chemistry* **288**:2805-2815.

Perez-Lloret S, Otero-Losada M, Toblli JE and Capani F (2017) Renin-angiotensin system as a potential target for new therapeutic approaches in Parkinson's disease. *Expert Opin Investig Drugs* **26**:1163-1173.

Poling A (2010) Progressive-ratio schedules and applied behavior analysis. *J Appl Behav Anal* **43**:347-349.

Rioult-Pedotti MS, Pekanovic A, Atiemo CO, Marshall J and Luft AR (2015) Dopamine Promotes Motor Cortex Plasticity and Motor Skill Learning via PLC Activation. *PloS one* **10**:e0124986.

Ross CA, MacCumber MW, Glatt CE and Snyder SH (1989) Brain phospholipase C isozymes: differential mRNA localizations by in situ hybridization. *Proc Natl Acad Sci U S A* **86**:2923-2927.

Saavedra JM (2016) Evidence to Consider Angiotensin II Receptor Blockers for the Treatment of Early Alzheimer's Disease. *Cell Mol Neurobiol* **36**:259-279.

Sim MS, Soga T, Pandy V, Wu YS, Parhar IS and Mohamed Z (2017) MicroRNA expression signature of methamphetamine use and addiction in the rat nucleus accumbens. *Metab Brain Dis* **32**:1767-1783.

Simanjuntak Y, Liang JJ, Lee YL and Lin YL (2017) Japanese Encephalitis Virus Exploits Dopamine D2 Receptor-phospholipase C to Target Dopaminergic Human Neuronal Cells. *Front Microbiol* **8**:651.

Sofuoglu M, DeVito EE, Waters AJ and Carroll KM (2013) Cognitive enhancement as a treatment for drug addictions. *Neuropharmacology* **64**:452-463.

Song MY, Makino A and Yuan JX (2011) Role of reactive oxygen species and redox in regulating the function of transient receptor potential channels. *Antioxid Redox Signal* **15**:1549-1565.

Tanaka O and Kondo H (1994) Localization of mRNAs for three novel members (beta 3, beta 4 and gamma 2) of phospholipase C family in mature rat brain. *Neurosci Lett* **182**:17-20.

Uramura K, Funahashi H, Muroya S, Shioda S, Takigawa M and Yada T (2001) Orexin-a activates phospholipase C- and protein kinase C-mediated Ca2+ signaling in dopamine neurons of the ventral tegmental area. *Neuroreport* **12**:1885-1889.

Vian J, Pereira C, Chavarria V, Kohler C, Stubbs B, Quevedo J, Kim SW, Carvalho AF, Berk M and Fernandes BS (2017) The renin-angiotensin system: a possible new target for depression. *BMC Med* **15**:144.

Villar-Cheda B, Rodriguez-Pallares J, Valenzuela R, Munoz A, Guerra MJ, Baltatu OC and Labandeira-Garcia JL (2010) Nigral and striatal regulation of angiotensin receptor expression by dopamine and angiotensin in rodents: implications for progression of Parkinson's disease. *Eur J Neurosci* **32**:1695-1706.

Watanabe MA, Kucenas S, Bowman TA, Ruhlman M and Knuepfer MM (2010) Angiotensin II and CRF receptors in the central nucleus of the amygdala mediate hemodynamic response variability to cocaine in conscious rats. *Brain Res* **1309**:53-65.

Wright JW and Harding JW (1994) Brain angiotensin receptor subtypes in the control of

physiological and behavioral responses. *Neurosci Biobehav Rev* **18**:21-53.

Yang YR, Kang DS, Lee C, Seok H, Follo MY, Cocco L and Suh PG (2016) Primary phospholipase C and brain disorders. *Advances in biological regulation* **61**:80-85.

Zhang X, Ping HY, Li JH, Duan SX and Jiang XW (2018) Diethylstilbestrol regulates mouse gubernaculum testis cell proliferation via PLC-Ca(2+) -CREB pathway. *Cell Biochem Funct* **36**:13-17.

Zhu L, Zhu J, Liu Y, Chen Y, Li Y, Chen S, Li T, Dang Y and Chen T (2015) Chronic methamphetamine regulates the expression of MicroRNAs and putative target genes in the nucleus accumbens of mice. *J Neurosci Res* **93**:1600-1610.

Zhuang S, Wang HF, Wang X, Li J and Xing CM (2016) The association of renin-angiotensin system blockade use with the risks of cognitive impairment of aging and Alzheimer's disease: A meta-analysis. *J Clin Neurosci* **33**:32-38.

Footnote page

This work was supported in part by the National Natural Science Foundation of China (81671323), the National Natural Science Foundation of Ningbo (2015A610188), K. C. Wong Magna Fund in Ningbo University, Zhejiang Provincial Key Laboratory of Pathophysiology (Ningbo University School of Medicine), and the Program for Innovative Research Team in Ningbo City (2015C110026).

Figure Legends

Figure 1: The effect of AT1R blockade on METH SA and cue-/drug- induced reinstatement

A: The effect of AT1R blockade on METH SA under the FR1 schedule. Increasing the dose of METH produced a significant decrease in drug infusions for all groups. Compared with the Saline+METH, DMSO+METH and 5CAN+METH groups, the 10CAN+METH group earned significantly fewer infusions of 0.025 and 0.05 mg/kg/infusion of METH following METH SA under the FR1 schedule (**p<0.01). B: The effect of AT1R blockade on METH SA under the PR schedule. Increasing the dose of METH produced a significant increase in breakpoints for all groups. The Saline+METH and DMSO+METH groups produced significantly higher breakpoints maintained by 0.075 mg/kg/infusion of METH than those of the 5CAN+METH ($^{\#}p$<0.05) and 10CAN+METH (**p<0.01) groups. Moreover, the 10CAN+METH rats produced significantly fewer breakpoints maintained by 0.1 mg/kg/infusion of METH than those of the Saline+METH, DMSO+METH and 5CAN+METH groups (p<0.01). C: The effect of AT1R blockade on cue-induced reinstatement of METH SA. Compared with the Saline and DMSO groups, the responses significantly decreased in the 5CAN (*p<0.05) and 10CAN (**p<0.01) groups. Group 5CAN showed a significant decrease in response, compared with group 10 CAN ($^{\#}p$<0.05). D: The effect of AT1R blockade on drug-induced reinstatement of METH SA. The responses significantly decreased in the 5CAN (*p<0.05) and 10CAN (**p<0.01) groups compared with those in the Saline and DMSO groups. Group 5CAN showed a significant decrease in

response, compared with group 10 CAN ($^{\#\#}p<0.01$).

Figure 2: Expression of D2R and AT1R of various brain regions in METH SA rats treated with CAN

A-C: Expressions of AT1R and D2R in various brain regions of rats self-administering METH under the FR1 schedule among group DMSO+METH, 5CAN+METH and 10 CAN+ METH (*$p<0.05$; **$p<0.01$; *** $p<0.001$). D-F: Expressions of AT1R and D2R in various brain regions of rats self-administering METH under the PR schedule among group DMSO+METH, 5CAN+METH and 10 CAN+ METH (**$p<0.01$).

Figure 3: Expression of D2R and AT1R in various brain regions of rats treated with CAN under the condition of cue-induced/drug-induced reinstatement of METH SA

A-C: Expressions of AT1R and D2R in various brain regions of rats receiving cue-induced reinstatement of METH SA test among group METH, SA, saline SA, DMSO and 10 CAN (**$p<0.01$). D-F: Expressions of AT1R and D2R in various brain regions of rats receiving drug-induced reinstatement of METH SA test among group METH, SA, saline SA, DMSO and 10 CAN. AT1R and D2R proteins compared with Beta actin as a standard of comparison (**$p<0.01$).

Figure 4: The effect of METH SA on miRNA expression targeting AT1R

A: METH SA rats exhibited stable performance of METH SA and earned an average of 87 infusions in each session. B: A hierarchical clustering map of NAc miRNAs for METH SA, yoked-METH and yoked-saline rats. Colors in the heat map indicate the correlation between the different data sets. C: 17 miRNAs associated with RAS were significantly changed in the NAc of METH SA rats, compared with yoked-METH and

yoked-saline rats (fold change $\geqslant$1.5, p< 0.05). D: a list of miRNAs with log2 value and fold changes. E: miR-219a-5p expression in NAc verified by RT-Qpcr (yoked-Saline group vs yoked- METH group, *** p<0.001, yoked-METH group vs METH-SA group, *** p<0.001).

Figure 5: The effect of miR-219a-5p overexpression in NAc on METH SA under the FR1 and PR schedule

A: The effects of NAc miR-219a-5p overexpression on METH SA under the FR1 schedule. The LV1-miR-219a-5p group earned significantly fewer infusions of 0.05, 0.075 and 0.1 mg/kg/infusion, compared with baseline and LV1NC groups (LV1NC vs. LV1-miR-219a-5p: ***p<0.001, **p<0.01, *p<0.05; baseline vs. LV1-miR-219a-5p: $^{###}p$<0.001). B: The expression of miR-219a-5p in the NAc was verified by RT-qPCR and was significantly higher in the LV1-219a-5p group than that in the LV1CN group following METH SA under the FR1 schedule (LV1NC vs. LV1-miR-219a-5p: *p<0.05). C: The effects of miR-219a-5p overexpression in the NAc on METH SA under the PR schedule, compared with baseline and LV1NC groups. The LV1NC and Baseline animals produced significantly higher breakpoints maintained by 0.05, 0.075 and 0.1 mg/kg/infusion of METH than those of the LV1-miR219a-5p group (LV1NC vs. LV1-miR-219a-5p: ***p<0.001; baseline vs. LV1-miR-219a-5p: $^{###}p$<0.001). D: The expression of miR-219a-5p in the NAc was verified by RT-qPCR and was significantly higher in the LV1-219a-5p group than that in the LV1NC group following METH SA under the PR schedule (LV1NC vs. LV1-miR-219a-5p: ***p<0.001).

Figure 6: The effect of NAc miR-219a-5p overexpression on cue and drug-induced

JPET Fast Forward. Published on March 13, 2019 as DOI: 10.1124/jpet.118.255729
This article has not been copyedited and formatted. The final version may differ from this version.

reinstatement of METH SA

A: The effect of miR-219a-5p overexpression on cue-induced reinstatement METH SA. The LV1CN rats exhibited significantly more responses than the LV1-miR-219a-5p rats (LV1NC vs. LV1-miR-219a-5p: $^{**}p<0.01$). B: NAc miR-219a-5p expression was verified via RT-qPCR following cue-induced reinstatement of METH SA. The NAc expression of miR-219a-5p in the LV1-219a-5p group was significantly higher than that in the LV1CN group following cue-induced reinstatement (LV1NC vs. LV1-miR-219a-5p: $^{***}p<0.001$). C: The effect of NAc miR-219a-5p overexpression on the drug-induced reinstatement of METH SA. The LV1-miR-219a-5p rats exhibited significantly fewer responses than the LV1CN rats ((LV1NC vs. LV1-miR-219a-5p: $^{**}p<0.01$). D: NAc miR-219a-5p expression was verified via RT-qPCR following drug-induced reinstatement of METH SA. The expression of NAc miR-219a-5p in the LV1-219a-5p group was significantly higher than that in the LV1CN group following drug-induced reinstatement of METH SA ((LV1NC vs. LV1-miR-219a-5p: $^{***}p<0.001$).

Figure 7: The effect of AT1R-PLCβ-CREB signaling pathway on the interaction between AT1R and METH SA

A: The levels of AT1R, PLCβ and CREB proteins were significantly decreased in rats with the overexpression of NAc miR-219a-5p, following METH SA under the FR1 schedule (LV1NC vs. LV1-miR-219a-5p: $^{*}p<0.05$). B: The levels of AT1R, PLCβ and CREB proteins were significantly decreased in rats with the overexpression of NAc miR-219a-5p, following METH SA under the PR schedule (LV1NC vs. LV1-miR-219a-5p: $^{*}p<0.05$). C: The levels of AT1R, PLC-β and CREB proteins were

significantly decreased in rats with the overexpression of NAc miR-219a-5p, following cue-induced reinstatement of METH SA (LV1NC vs. LV1-miR-219a-5p: *p<0.05; **p<0.01). The levels of AT1R, PLC-β and CREB proteins were significantly decreased in rats with the overexpression of NAc miR-219a-5p, following cue-induced reinstatement of METH SA (LV1NC vs. LV1-miR-219a-5p: *p<0.05; **p<0.01; ***p<0.001).

Figure 8: Changes of AT1R/PLCβ/CREB protein and mRNA expression following METH and CAN treatment in PC12 cells

A: Representative image of AT1R/PLCβ/CREB protein expression in PC12 cells treated with METH and CAN. B-D: Changes of AT1R/PLCβ/CREB protein expression in PC12 cells treated with METH and CAN (***p < 0.001). E-G: mRNA levels of Agtr1b, PLCβ1 and CREB1 in PC12 cells treated with METH and CAN (* p<0.05; ** p<0.01; *** p<0.001).

Figure 9

The AT1R-PLCβ-CREB signaling pathways

Angiotensin II binds to AT1R. The activation of AT1R results the cleavage of inositol triphosphate (IP_3) and diacylglycerol (DAG) from PLCβ. IP_3 increases the flow of Ca^{2+} into the Endoplasmic Reticulum (ER) and increases the concentration of Ca^{2+}. DAG activates protein kinase C (PKC), which subsequently activates CREB via phosphorylation.

JPET Fast Forward. Published on March 13, 2019 as DOI: 10.1124/jpet.118.255729
This article has not been copyedited and formatted. The final version may differ from this version.

Figure 1

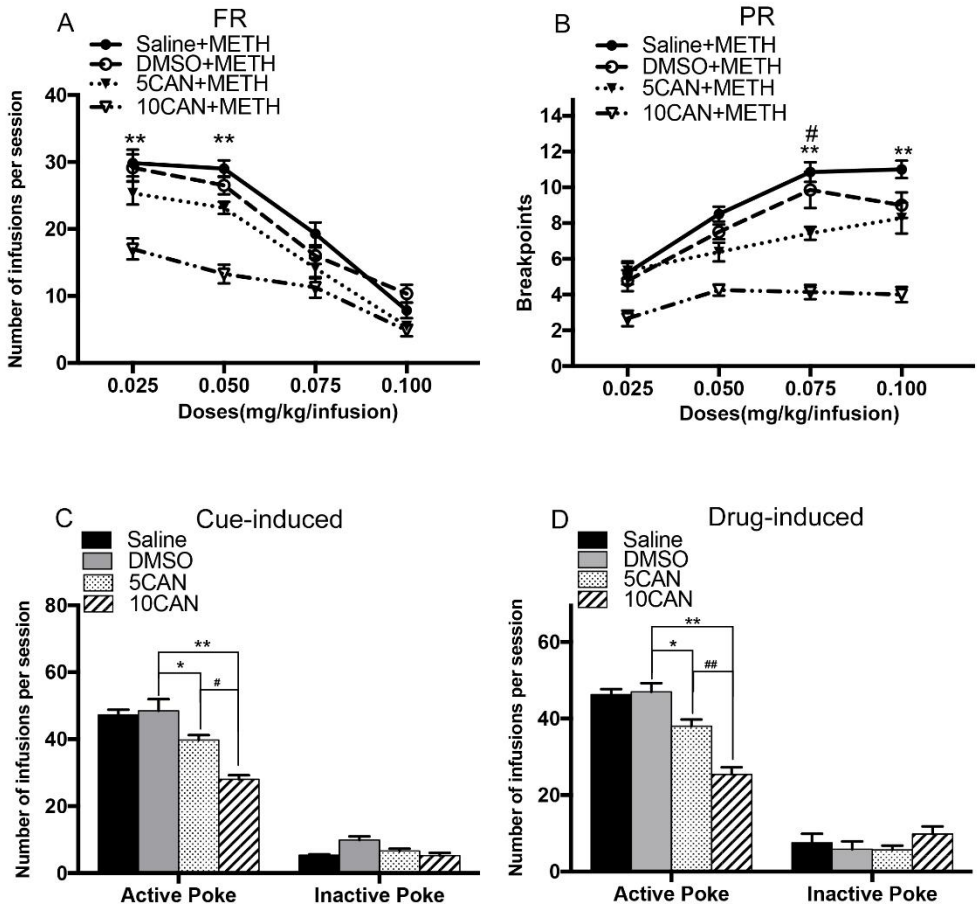

JPET Fast Forward. Published on March 13, 2019 as DOI: 10.1124/jpet.118.255729
This article has not been copyedited and formatted. The final version may differ from this version.

Figure 2

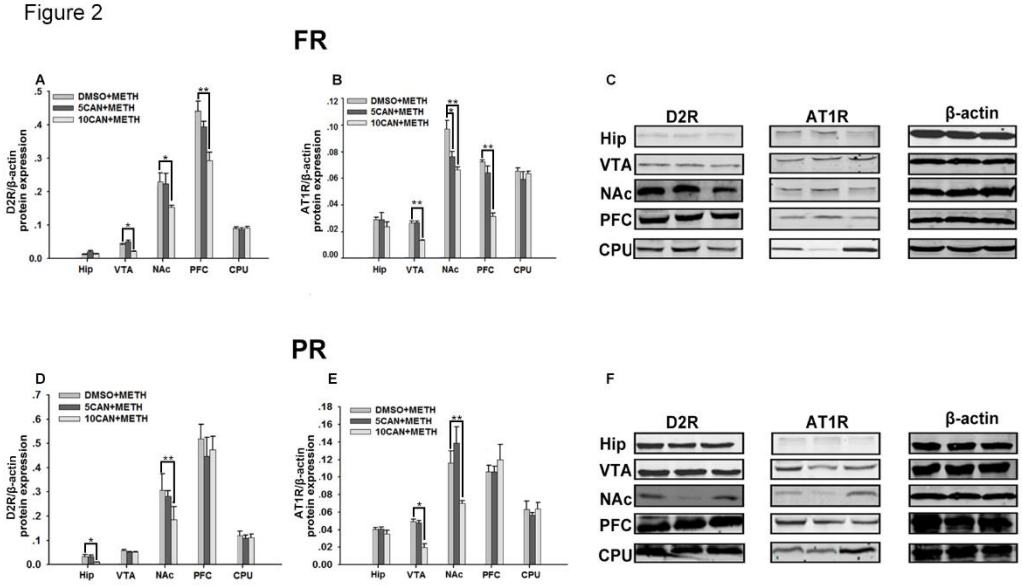

JPET Fast Forward. Published on March 13, 2019 as DOI: 10.1124/jpet.118.255729
This article has not been copyedited and formatted. The final version may differ from this version.

Figure 3

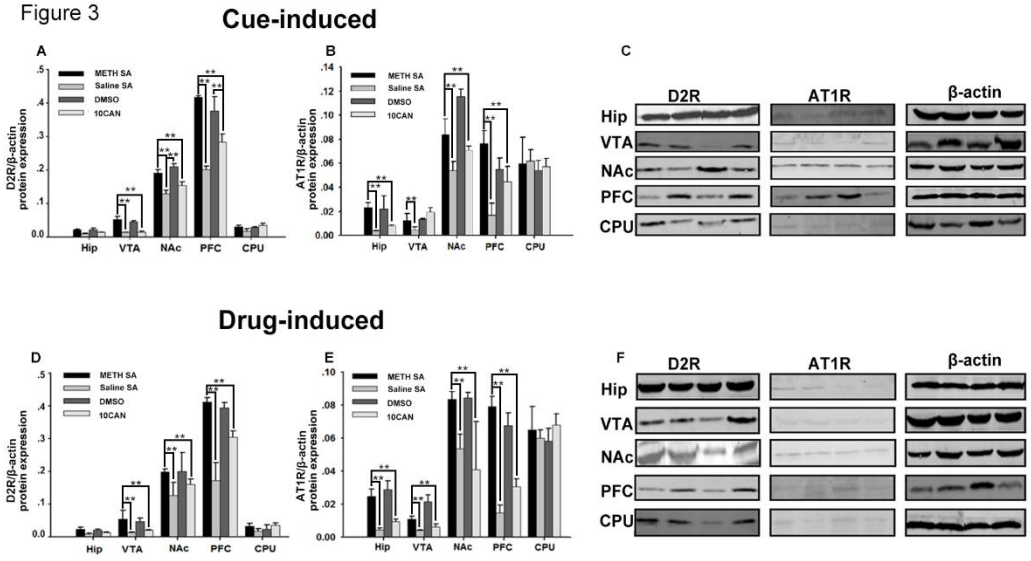

JPET Fast Forward. Published on March 13, 2019 as DOI: 10.1124/jpet.118.255729
This article has not been copyedited and formatted. The final version may differ from this version.

Figure 4

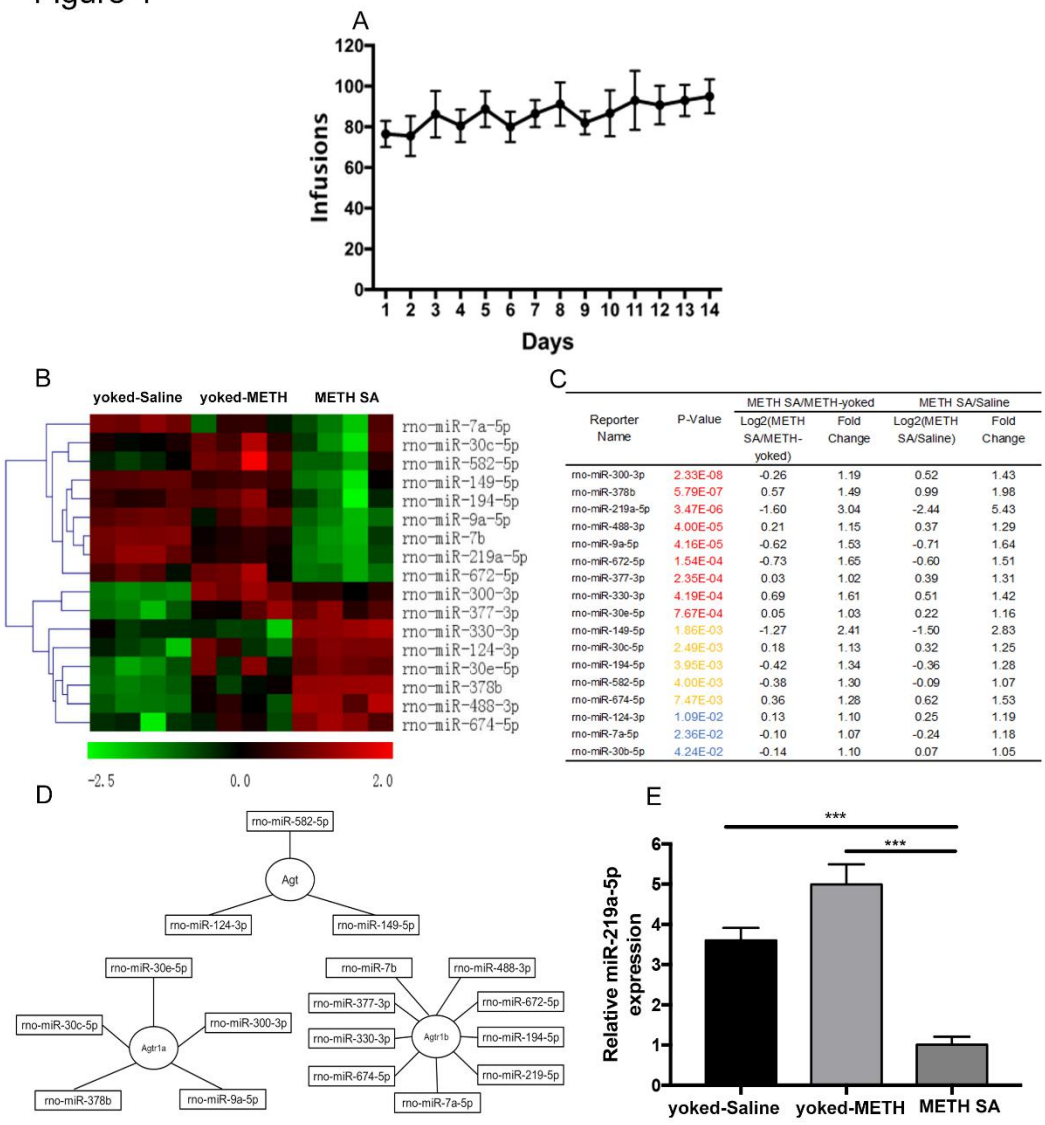

Reporter Name	P-Value	METH SA/METH-yoked Log2(METH SA/METH-yoked)	METH SA/METH-yoked Fold Change	METH SA/Saline Log2(METH SA/Saline)	METH SA/Saline Fold Change
rno-miR-300-3p	2.33E-08	-0.26	1.19	0.52	1.43
rno-miR-378b	5.79E-07	0.57	1.49	0.99	1.98
rno-miR-219a-5p	3.47E-06	-1.60	3.04	-2.44	5.43
rno-miR-488-3p	4.00E-05	0.21	1.15	0.37	1.29
rno-miR-9a-5p	4.16E-05	-0.62	1.53	-0.71	1.64
rno-miR-672-5p	1.54E-04	-0.73	1.65	-0.60	1.51
rno-miR-377-3p	2.35E-04	0.03	1.02	0.39	1.31
rno-miR-330-3p	4.19E-04	0.69	1.61	0.51	1.42
rno-miR-30e-5p	7.67E-04	0.05	1.03	0.22	1.16
rno-miR-149-5p	1.86E-03	-1.27	2.41	-1.50	2.83
rno-miR-30c-5p	2.49E-03	0.18	1.13	0.32	1.25
rno-miR-194-5p	3.95E-03	-0.42	1.34	-0.36	1.28
rno-miR-582-5p	4.00E-03	-0.38	1.30	-0.09	1.07
rno-miR-674-5p	7.47E-03	0.36	1.28	0.62	1.53
rno-miR-124-3p	1.09E-02	0.13	1.10	0.25	1.19
rno-miR-7a-5p	2.36E-02	-0.10	1.07	-0.24	1.18
rno-miR-30b-5p	4.24E-02	-0.14	1.10	0.07	1.05

JPET Fast Forward. Published on March 13, 2019 as DOI: 10.1124/jpet.118.255729
This article has not been copyedited and formatted. The final version may differ from this version.

Figure 5

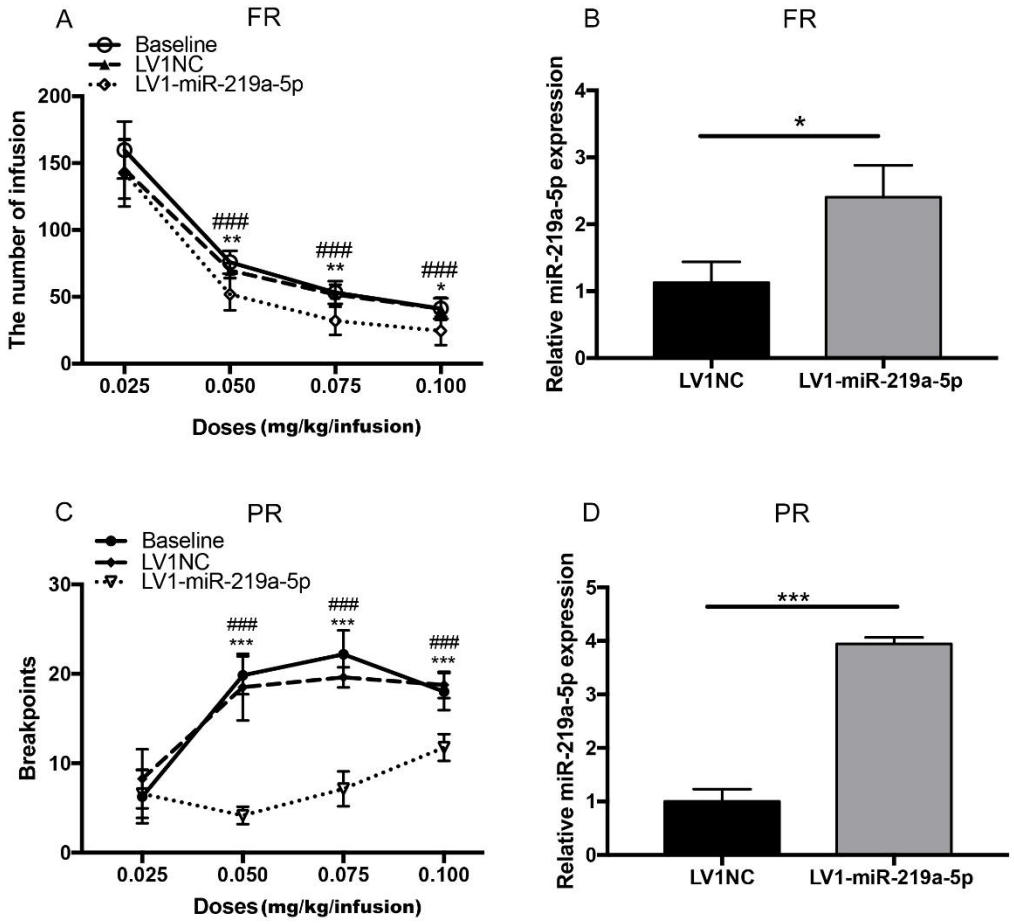

JPET Fast Forward. Published on March 13, 2019 as DOI: 10.1124/jpet.118.255729
This article has not been copyedited and formatted. The final version may differ from this version.

Figure 6

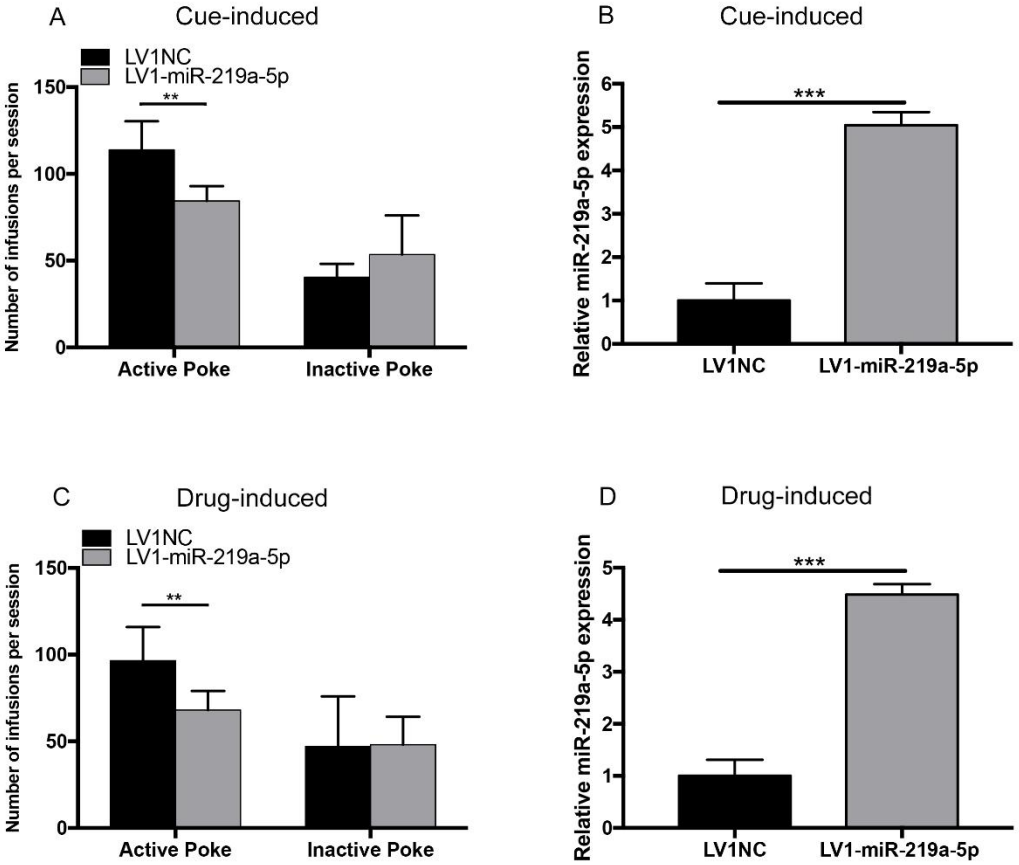

JPET Fast Forward. Published on March 13, 2019 as DOI: 10.1124/jpet.118.255729
This article has not been copyedited and formatted. The final version may differ from this version.

Figure 7

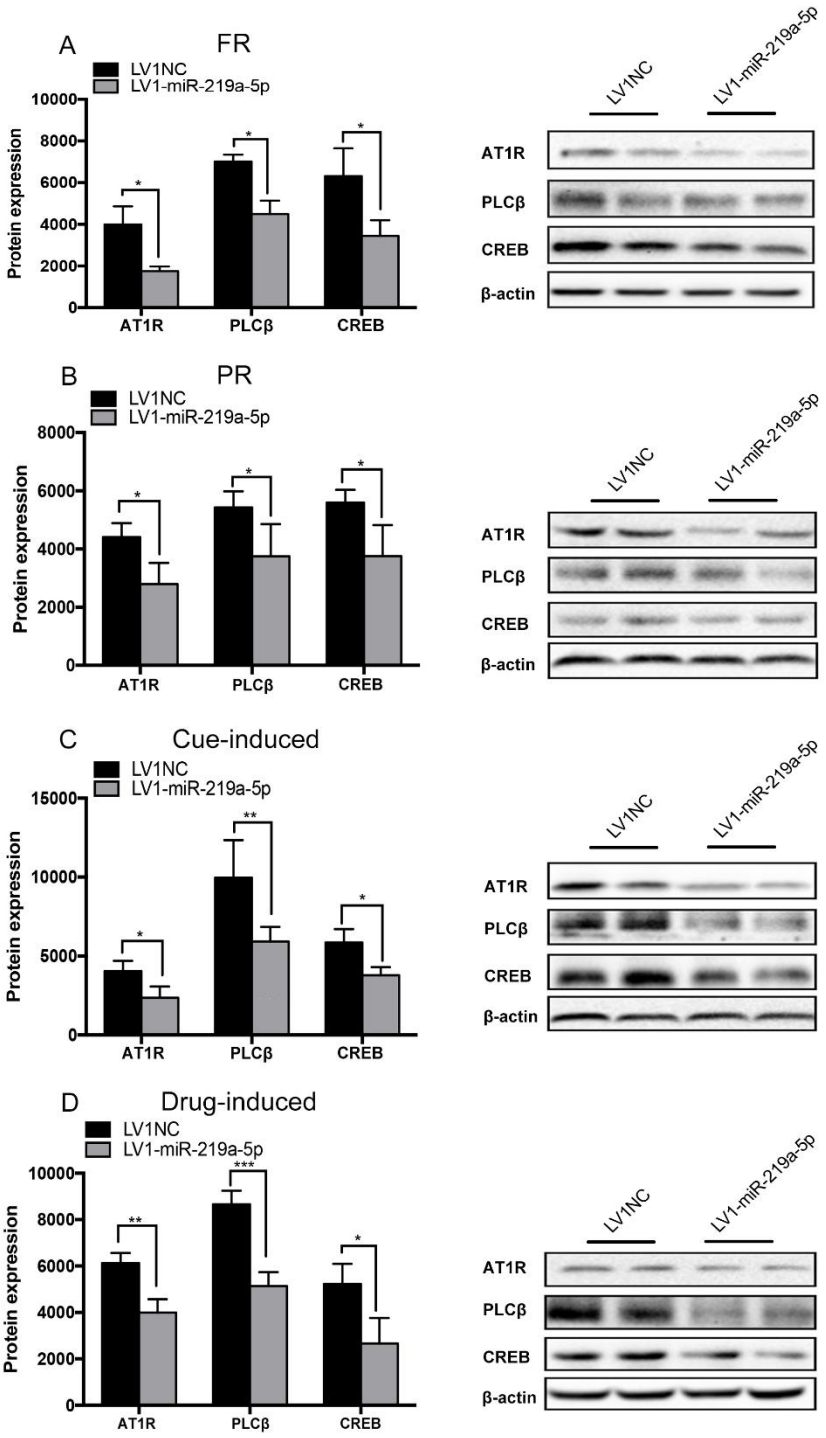

Figure 8

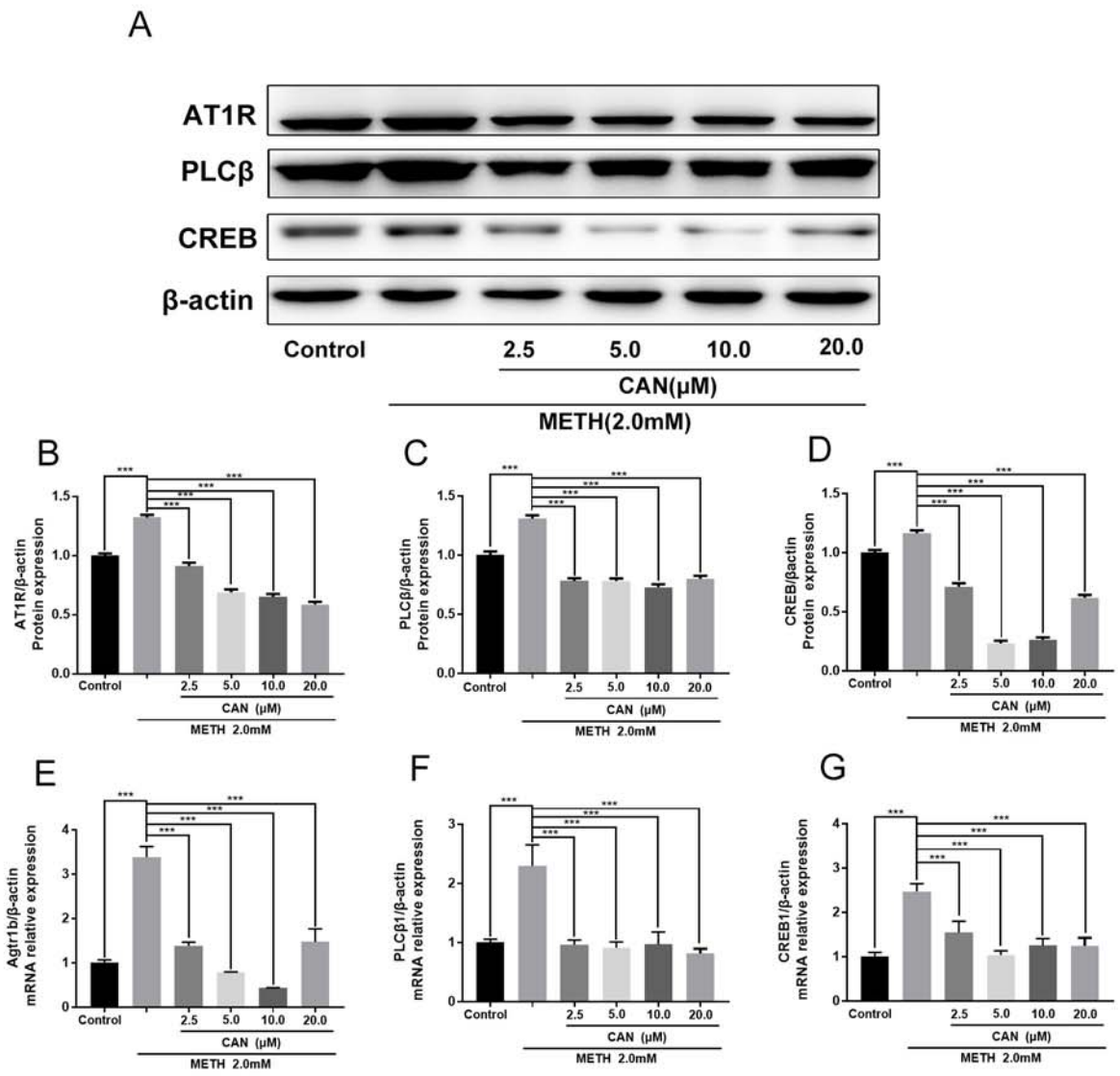

JPET Fast Forward. Published on March 13, 2019 as DOI: 10.1124/jpet.118.255729
This article has not been copyedited and formatted. The final version may differ from this version.

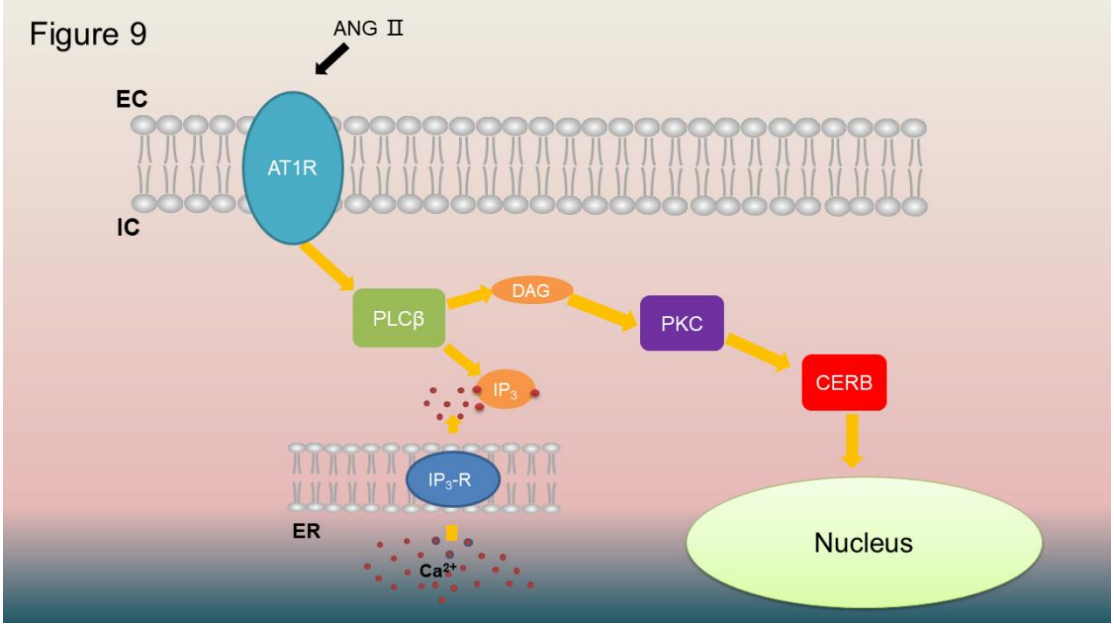

JPET # 255729

Inhibition of methamphetamine self-administration and reinstatement by central blockade of angiotensin II receptor in rats

[1]Xing Xu, [1]Jian Pan, [2]Xingxing Li, [3]Yan Cui, [1]Zijuan Mao, [1]Boliang Wu, [3]Huachong Xu, [1,4]Wenhua Zhou, [1]Yu Liu

[1] Ningbo University School of Medicine, 818 Fenghua Road, Ningbo, Zhejiang 315211, P. R. China

[2] Ningbo Kangning Hospital, 1 South Zhuangyu Road, Ningbo, Zhejiang 315201, P. R. China.

[3] Ningbo Public Security Bureau Ningbo Anti-drug Office, 36 Xibei Road, Zhejiang 315040, P. R. China

[4] Ningbo Addiction Research and Treatment Center, 21 Xibei Road, Zhejiang 315040, P. R. China

Table 1. Primer Sequences of Relevant Genes Designed for qPCR

Genes	Forward primer	Reverse primer	Product length (bp)
rno-miR-219a-5p	CTGATTCCCTGATTGTCCAAAC	TATGCTTGTTCTCGTCTCTGTGTC	70
U6	CAGCACATATACTAAAATTGGAACG	ACGAATTTGCGTGTCATCC	76
β- actin	CTATCCTGGCCTCACTGTCC	ACAGTCCGCCTAGAAGCATT	107
Agtr1b	CAATCTGGCTGTGGCTGACTT	TGCACATCACAGGTCCAAAGA	101
PLCβ1	TGTCTCCCGAGGCTCTACAA	TAGTAAGCGGGACTACACGC	108
Creb1	TGCAGACATTAACCATGACCA	GTTGCTGGGCACTAGAATCTG	104

Figure 1

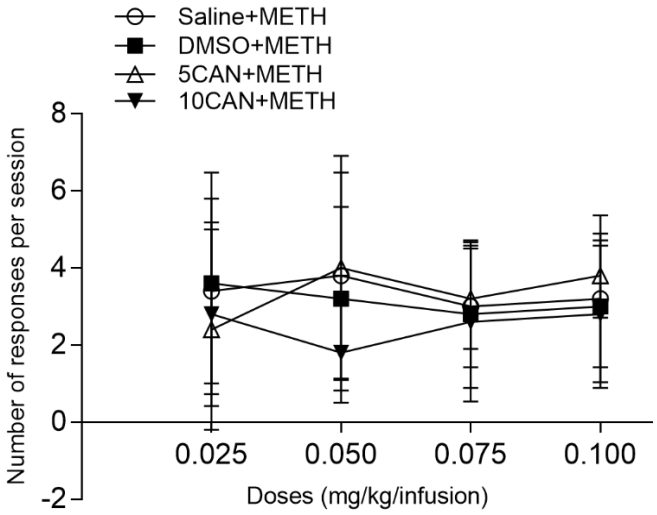

TWO-way repeated measure ANOVA was used to analyze the effect of 5 and 10 CAN on inactive nose-poke responses during the period of METH SA under FR1 schedule. There was no major effect of Group ($F_{(3, 64)} = 0.089$, $p=0.966$), Dose ($F_{(3, 64)} = 0.702$, $p=0.554$) and Group X Dose interaction ($F_{(9, 64)} = 0.322$, $p=0.965$).

Figure 2

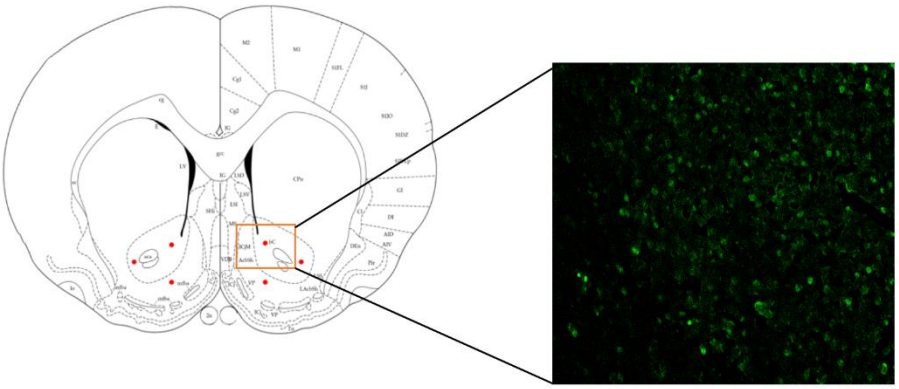

Following the micro-injection, the injection site of NAc for each animal was examined by a fluorescence microscope.Red circles in left panel are locations at which viral infusions were targeted in NAc. The right panel is the visualized overexpression of miR-219a-5p (shown by arrow) in LV1-miR-219a-5p rats. No infusion was found. The image is now included as the supplementary material.